Received: 23 February 2023 | Revised: 25 July 2023 | Accepted: 31 July 2023

DOI: 10.1111/pce.14685

ORIGINAL ARTICLE

Plant, Cell & Environment | WILEY

Enhanced meristem development, tolerance to oxidative stress and hyposensitivity to nitric oxide in the hypermorphic *vq10-H* mutant in *AtVQ10* gene

Beatriz Gayubas | **Mari-Cruz Castillo** | **Sara Ramos** | **José León**

Instituto de Biología Molecular y Celular de Plantas (Consejo Superior de Investigaciones Científicas—Universidad Politécnica de Valencia), Valencia, Spain

Correspondence
José León, Instituto de Biología Molecular y Celular de Plantas (Consejo Superior de Investigaciones Científicas—Universidad Politécnica de Valencia), Valencia, Spain.
Email: jleon@ibmcp.upv.es

Funding information
Spanish Ministry of Economy and Competitiveness and "Agencia Estatal de Investigación"/FEDER/European Union, Grant/Award Numbers: BIO2017-82945-P, PID2020-112618GB-I00; Generalitat Valenciana/FEDER, Grant/Award Number: IDIFEDER/2021/007; Ministerio de Ciencia e Innovación contract, Grant/Award Number: PRE2018-086290

Abstract

Nitric oxide (NO) and reactive oxygen are common factors in multiple plant responses to stress, and their involvement in hypoxia-triggered responses is key to ensure growth under adverse environmental conditions. Here, we analyse the regulatory functions exerted by hypoxia-, NO- and oxidative stress-inducible *Arabidopsis* gene coding for the VQ motif-containing protein 10 (VQ10). A hypermorphic *vq10-H* mutant allowed identifying VQ10-exerted regulation on root and shoot development as well as its role in regulating responses to NO and oxidative stress. Enhanced *VQ10* expression in *vq10-H* plants led to enhanced elongation of the primary root, and increased root cell division and meristem size during early postgermination development. In shoots, VQ10 activation of cell division was counteracted by WRKY33-exerted repression, thus leading to a dwarf bushy phenotype in plants with enhanced *VQ10* expression in a *wrky33* knock-out background. Low number of differentially expressed genes were identified when *vq10-H* versus Col-0 plants were compared either under normoxia or hypoxia. *vq10-H* and *VQ10ox* plants displayed less tolerance to submergence but, in turn, were more tolerant to oxidative stress and less sensitive to NO than wild-type plants. VQ10 could be a node integrating redox-related regulation on development and stress responses.

KEYWORDS
Arabidopsis thaliana, hypermorphic mutant, root and shoot development, VQ protein

1 | INTRODUCTION

VQ proteins, defined as those containing a sequence motif with a core five conserved amino acids FxxhVQxhTG, were initially considered as plant-specific transcriptional regulators (Jing & Lin, 2015). However, it has been recently reported that VQ proteins are an ancient nonplant-specific family with varying numbers of VQs identified in moss, gymnosperm and angiosperm plants as well as in some of fungi, nematodes and bacteria (Jiang et al., 2018). The genome of model organisms for monocots (rice) and dicots (Arabidopsis) contained 40 and 34 VQ protein-encoding genes, respectively (Cheng et al., 2012; Kim et al., 2013; Xie et al., 2010). VQ proteins play diverse regulatory roles on developmental and stress-related responses. Among different stresses, VQ proteins regulate

the responses to high (Ding et al., 2019) and low (Ye et al., 2016) temperatures; defense against pathogens (Le Berre et al., 2017; Jiang & Yu, 2016; Kim et al., 2013) and against generalist herbivores (Ali et al., 2019) and salt and drought stress (Hu et al., 2013; Kim et al., 2013; Song et al., 2016). Developmental traits such as pollen development, germination and tube growth (Lei et al., 2017, 2018); seed development (Garcia et al., 2003), germination (Pan et al., 2018) and size (Wang et al., 2010); seedling deetiolation (Li, Jing, et al., 2014) and vegetative growth and flowering time (Gargul et al., 2015) are all regulated by VQ proteins. However, the function of most of the members of the Arabidopsis family remains poorly known.

Although is widely established that VQ proteins behave as regulatory elements in gene expression, it is not so clear whether they act as transcriptional regulators or just as interactors/modulators of true transcription factors such as those of the WRKY family (Cheng et al., 2012). Most of the Arabidopsis VQ proteins have transcriptional regulatory activity, some displaying activating functions, while some others act as transcriptional repressors (Jing & Lin, 2015). In addition, for some of these proteins, such as VQ4/MVQ1 and VQ29, which function as transcriptional repressors, it has been shown that their regulatory activity requires the integrity of the VQ domain (Li, Li, et al., 2014; Weyhe et al., 2014). Among the few Arabidopsis VQ proteins that did not display regulation on transcriptional activity (Jing & Lin, 2015), VQ10 has been just characterised as a regulator of Arabidopsis defense against the necrotrophic fungus *Botrytis cinerea* (Chen et al., 2018), and as one of the five Arabidopsis *VQ* genes coregulated by hypoxia, nitric oxide (NO) and oxidative stress (León et al., 2021), conditions that coexist during plants responses to limited oxygen availability. Plants usually grow and thrive in a normoxic environment containing about 21% O_2. However, sometimes plants experience hypoxic environments and they do not have a system allowing O_2 to be distributed throughout the body, as animals do through haemoglobin in the blood. In turn, it diffuses from tissue to tissue or is transported through tissues through the vascular system in plants (Armstrong et al., 2006). Hypoxic conditions can be imposed to plants by environmental factors, such as torrential rains and subsequent flooding that keep plants submerged for variable periods of time (Voesenek & Bailey-Serres, 2015), or by endogenous factors, such as high metabolic rates demanding high O_2 consumption (Considine et al., 2017). To improve tolerance to limiting O_2 conditions, plants have developed enormous plasticity adopting changes in their physiology and metabolism (Bailey-Serres & Voesenek, 2008; Voesenek & Bailey-Serres, 2013), or even involving morphological changes or creating new organs such as the aerenchyma (Takahashi et al., 2015). The transition from a normoxic to a hypoxic condition involves multiple responses that include physiological, molecular and metabolic changes in plant cells. Many of the alterations in gene expression experienced by hypoxic plants are regulated by the function of group VII transcription factors of the ERF/AP2 family (ERFVIIs), which stability is controlled through an N-terminal sequence-dependent proteolytic process, the Cys/Arg N-degron pathway that is strictly dependent on NO and O_2 (Gibbs et al., 2014), thus representing an important node in O_2- and NO-mediated signalling and a key process in plant responses to hypoxia.

Here we address the functional and molecular characterisation of the hypoxia-, NO- and oxidative stress-inducible *VQ10* gene, and the regulatory role exerted by the encoded protein on meristem development as well as on the sensitivity to hypoxia, NO and oxidative stress.

2 | MATERIALS AND METHODS

2.1 | Plant growth conditions and materials

Arabidopsis (*Arabidopsis thaliana*) seeds were surface sterilised with chlorine gas before sowing in murashige skoog (MS) (Duchefa Biochemie) medium plates containing 1% (w/v) sucrose. Seeds from wild-type Col-0 and *vq10-H* (SAIL_23_A10C1) and *glb1* (SAIL_100_F11) genotypes were obtained from Nottingham Arabidopsis Stock Center (NASC). *wrky33* seeds (GK_324G011) were kindly supplied by Prof. Imre Somssich (Max Planck Institute for Plant Breeding Research). Reporter *cycB1;1:GUS* line in Col-0 background (Colon-Carmona et al., 1999) were used to generate reporter lines in *vq10-H* and *wrky33* backgrounds by genetic crosses of the corresponding genotypes followed by selection with kanamycin and the subsequent genotyping by PCR with specific oligonucleotides (Supporting Information: Table S1). Plants confirmed to be double homozygous for the transgene and mutation were used for subsequent β-glucuronidase (GUS) staining according to previously reported protocol (Weigel & Glazebrook, 2002). *vq10-H* and *wrky33* mutant plants were also genetically crossed and the progeny genotyped by PCR with specific primers (Supporting Information: Table S1). Plants overexpressing N-terminal 3×HA-tagged versions of VQ10 and GLB1 were generated by Gateway subcloning of the full-length complementary DNAs (cDNAs) cloned in *pCR8* TOPO vector, in *pAlligator2* binary vector that allows selection of transformed plants by screening fluorescent seeds (Bensmihen et al., 2004). After transformation of *Agrobacterium tumefaciens* C58 with the corresponding constructs, Col-0 plants were genetically transformed by dipping floral organs in a suspension of transformed Agrobacterium (Clough & Bent, 1998), and selected for homozygous plants.

To test the tolerance to oxidative stress, seeds of the same age of the different genotypes were sown in water in 24-well plates and maintained under photoperiodic conditions (16 h light:8 h darkness; 100 μmol m^{-2} s^{-1}) at 21°C and supplemented with paraquat/methyl viologen (0.1 or 0.2 mM) or without paraquat/methyl viologen as control. Seed germination rates were calculated at the indicated times as the mean of three independent experiments with around 50 seeds per genotype and condition.

Experiments under hypoxic conditions were performed by incubation in a box containing an inlet for N_2 gas and an O_2 sensor connected to a ProOx Model 110 controller that allows tight control of the O_2 concentration inside the box (BioSpherix). In vitro 12-day-old plants grown under long-day photoperiodic conditions in

Murashige Skoog medium supplemented with 1% (w/v) sucrose were exposed to hypoxia treatment under low light intensity (20 µmol m^{-2} s^{-1}) or darkness, as indicated, at 1% (v/v) O_2 for the indicated time. Samples were collected right after finishing the hypoxia treatment and frozen in liquid nitrogen for RNA extraction. Submergence experiments were performed with 4-week-old plants completely submerged (plants were 15 cm below water surface) in water-filled tanks pre-equilibrated at 21°C in darkness. After 3 days under submergence, plants were removed from the water and recovered under standard growing conditions for 15 days.

NO sensitivity was analysed by a hypocotyl shortening assay with etiolated plants as previously described (Castillo et al., 2018). Briefly, seeds of the different genotypes were sown in mass spectrometry (MS)-2-(N-morpholino)ethanesulfonic acid plates, stratified at 4°C under darkness for 4 days, then activated for germination by exposure to light for 6 h, and then incubated inside tightly sealed chambers injected with 300 ppm NO for 4 days under darkness. After that, etiolated seedlings were scanned to quantify the hypocotyl length using ImageJ. Values were compared to control etiolated seedlings not exposed to NO.

2.2 | RNA isolation, qRT-PCR and RNA-Seq analysis

RNA was extracted and purified with Nucleospin RNA Plant kit (Macherey-Nagel), reverse-transcribed with M-MuLV Reverse transcriptase (RNase H minus from Nzytech) and oligo-dT, and the resulting cDNA was quantified by real-time PCR with an Applied Biosystems QuantStudioTM 3 PCR system by using specific primer pairs (Supporting Information: Table S1) for *VQ10* (*AT1G78410*), *WRKY33* (*AT2G38470*), *PDC1* (*AT4G33070*), *LBD41* (*AT3G02550*), *GLB1* (*AT2G16060*) and the reference genes *TIP41L* (*AT4G34270*) and *ACTIN2* (*At3g18780*) as reported before (Castillo et al., 2008; Czechowski et al., 2005).

A genome-wide transcriptome analysis of 12-day-old wild-type (Col-0) and *vq10-H* mutant plants, either grown under normoxic (21% O_2) conditions or grown under normoxia and then submitted to hypoxia (1% O_2) for 4 h, was performed by RNA-Seq (BGI Tech Solutions). Libraries were prepared from oligo-dT enriched mRNAs obtained from total RNAs with RNA integrity number > 8.0 as analysed by a 2100 Bioanalyzer (Agilent Technologies Inc.). RNA was fragmented, then first-strand cDNA was generated using random N6-primed reverse transcription, followed by second-strand cDNA synthesis with dUTP instead of dTTP. The synthesised cDNAs were subjected to end-repair and then was 3′ adenylated. Adaptors were ligated to the ends of these 3′ adenylated cDNA fragments, and before PCR amplification, the dUTP-marked strand is selectively degraded by Uracil-DNA-Glycosylase (UDG). The remaining strand is amplified to generate a cDNA library suitable for sequencing. After denaturing the PCR product by heat, the single stranded DNA is cyclized by splint oligo and DNA ligase, the DNA nanoball synthesis was performed and finally, sequencing was performed with DNBSEQ Technology platform. Raw data were filtered with SOAPnuke (v.1.5.2) software (with -l 15 -q 0.2 -n 0.05 parameters) developed by BGI. The filtered clean reads were saved in FASTQ format. Reference genome alignment was performed by Hierarchical Indexing for Spliced Alignment of Transcripts (HISTAT) software (v.2.0.4; Parameters: --sensitive --no-discordant --no-mixed -I 1 -X 1000 -p 8 --rna-strandness RF).

2.3 | Analysis of root growth, cell division and meristem size

The root length was calculated by using Image J2/Fiji from images of vertically grown plants. The size of root meristems was calculated from images of propidium iodide-stained roots of 4-day-old plants obtained by confocal microscopy with AxioObserver Zeiss LSM 780 confocal microscope (with excitation at 561 nm and emission at 578–670 nm range with a peak at 625 nm). The number of cells from the quiescent centre (QC) to the first cell duplicating the size of the previous one was assigned as meristem size as previously reported (Perilli & Sabatini, 2010). Values are the mean ± standard error of five to eight roots per genotype. Cell division in the root meristem zone was monitored by using the *cycB1;1:GUS* reporter line that has been extensively used before for this purpose (Colon-Carmona et al., 1999).

2.4 | Analysis of the starch content

Starch content was visualised by the staining of 6-day-old plants with Lugol's iodine reagent (Sigma-Merck). After washings, stained plants were visualised and photographed with a Nikon Eclipse E600 microscope.

2.5 | In silico analyses and predictions

Gene Ontology (GO) Consortium tools (http://www.geneontology.org) and PANTHER (http://go.pantherdb.org/) were used to analyse the enrichment of functional categories, and AtCAST3.1 (http://atpbasmd.yokohama-cu.ac.jp/cgi/atcast/search_input.cgi) and Arabidopsis RNA-Seq Database (http://ipf.sustech.edu.cn/pub/athrna/) were used to compare available transcriptome datasets. Gene lists overlapping was analysed by Venny 2.1.0 (https://bioinfogp.cnb.csic.es/tools/venny/index.html).

2.6 | Statistical analyses

The values of transcript levels, root lengths, meristem size and seed germination rates are presented as the mean of at least three independent biological replicates ± SE. Statistical significance was analysed as indicated in the figure legends by unpaired Student's *t* test comparing any mutant genotype to the wild-type Col-0 values

or any condition to the control untreated set. When comparisons involved two variables, a two-way analysis of variance was used as indicated. Statistical significance with $p < 0.05^{*}$, $p < 0.005^{**}$ and $p < 0.001^{***}$ are shown.

2.7 | Quantification of endogenous ATP levels

ATP levels were quantified by the fluorometric ATP Assay Kit (Sigma-Aldrich Merck) from 14-day-old Arabidopsis seedlings that were homogenised to fine powder in liquid nitrogen. Three biological independent replicates with two technical replicates each were analysed.

2.8 | Analysis of protein-bound and free 3-nitrotyrosine

Protein-bound 3-nitrotyrosine was analysed by Western blot with anti-3-nitrotyrosine antibodies (Cayman Chemicals) at 1:1000 dilution in tween-tris buffered saline. Total protein was extracted from 14-day-old Arabidopsis seedlings exposed to 300 ppm NO for 10 min and recovered for 6 h or untreated as control. Equal loading of lanes was assessed by Ponceau S-staining of nitrocellulose membranes. For free 3-nitrotyrosine quantification by ultra performance liquid chromatography (UPLC)-MS/MS, samples (100 mg of 14-day-old whole seedlings), either treated or untreated as mentioned above, were homogenised with liquid nitrogen and extracted in 600 µL 100% methanol, supplemented with 1 ppm genistein as internal standard, for 15 min at 70°C. After extraction and centrifugation for 10 min at 14 000 rpms, 500 µL of the supernatant were transferred to a new vial. Then 250 µL of $CHCl_3$ and 500 µL of water supplemented with 1 ppm Genistein were added. The mixture was vortexed for 15 s and centrifuged for 15 min at 14 000 rpms. The aqueous phase was filtered with a 0.2 µM filter and 5 µL were injected. Three replicates of each genotype and treatment were analysed. The analysis was performed using an Orbitrap Exploris 120 mass spectrometer coupled with a Vanquish UHPLC System (Thermo Fisher Scientific). LC was carried out by reverse-phase ultraperformance liquid chromatography using an Acquity PREMIER BEH C18 UPLC column (1.7 µM particle size, dimensions 2.1 × 150 mm) (Waters Corp.). Mobile phases were 0.1% formic acid in water (phase A), and 0.1% formic acid in acetonitrile (phase B). The gradient programme was conditioned as follows: 0.5% solvent B over the first 2 min, 0.5%–30% solvent B over 25 min, 30%–100% solvent B over 13 min, 2 min at 100% B, return to the initial 0.5% solvent B over 1 min and conditioning at 0.5% B for 2 min. The flow rate was 0.4 mL/min and the column temperature was set at 40°C. Ionisation was performed with heated electrospray ionisation (H-ESI) in positive mode. Samples were acquired in full scan mode (resolution set at 120 000 measured at full width at half maximum). To identify 3-nitrotyrosine an authentic standard was used (Merck). Free 3-nitrotyrosine analysis was performed at the IBMCP Metabolomics Platform (UPV-CSIC).

3 | RESULTS

3.1 | Identification and molecular characterisation of a hypermorphic mutant for *VQ10* gene

Arabidopsis *VQ10* gene (*At1g78410*) was identified through in silico search as a target of coregulation by hypoxia, NO and oxidative stress (León et al., 2021). A search in public transcriptome databases suggested that *VQ10* gene was regulated by multiple environmental, developmental and nutritional factors (Figure 1a). Among them, *VQ10* expression was maximum in 40-day-old leaves when senescence is already set up, and also in 2-week-old younger seedlings upon oxidative stress triggered by exposure to ozone (Figure 1a). We confirmed that *VQ10* gene was transiently upregulated peaking at 30 min after hypoxia or NO treatment (Figure 1b).

The public seed banks of Arabidopsis insertional mutants were browsed to identify a knock-out mutant for this gene. The insertional mutant SAIL_23_A10C1, originally annotated in the T-DNA express SIGnAL website (http://signal.salk.edu/) as a T-DNA insertion in the *VQ10* exon (Figure 2a), was instead inserted in the 3′-untranslated region (UTR) region, as demonstrated by PCR with gDNA from wild type and mutant plants and with specific primers of the coding sequence and the 3′-UTR region (Figure 2b). T-DNA insertion did not lead to reduced levels of *VQ10* transcripts, but instead to 3.5- and 1.8-fold increase in transcript levels when compared homozygous and heterozygous mutant, respectively, to wild-type plants (Figure 2c), thus indicating this mutant allele, which we named *vq10-H*, is a hypermorphic mutant. No obvious developmental phenotype was observed either in heterozygous or homozygous mutant plants.

3.2 | Differentially expressed transcriptomes in *vq10-H* plants under normoxia and hypoxia

Since *VQ10* gene was rapidly induced by hypoxia (Figure 1b), we decided to analyse the genome-wide effect of the hypermorphic *vq10-H* mutation on the transcriptome of plants under normoxic and hypoxic conditions. RNA-Seq analyses were performed (Supporting Information: Table S2) for Col-0 and *vq10-H* plants either grown under normoxia or in normoxic-grown plants submitted to a 4 h period of 1% O_2, when transient hypoxia-induced expression of *VQ10* gene had already occurred (Figure 1b). A comparison of the mutant genotype with wild-type Col-0 background allowed identifying differentially expressed genes (DEGs) under normoxia (Table 1) or hypoxia (Table 2). The impact on differential gene expression of *vq10-H* mutation (Figure 3a) was significantly shorter than the effect of hypoxia (Figure 3b). Just 26 and 24 DEGs were identified when comparing *vq10-H* versus Col-0 under normoxia or hypoxia, respectively (Tables 1 and 2). Correlating with the increased *VQ10* transcript levels, we identified several loci close to *At1g78410* (*VQ10* gene) in chromosome 1 that were strongly downregulated in *vq10-H* plants either in normoxia or hypoxia (Tables 1 and 2). This gene

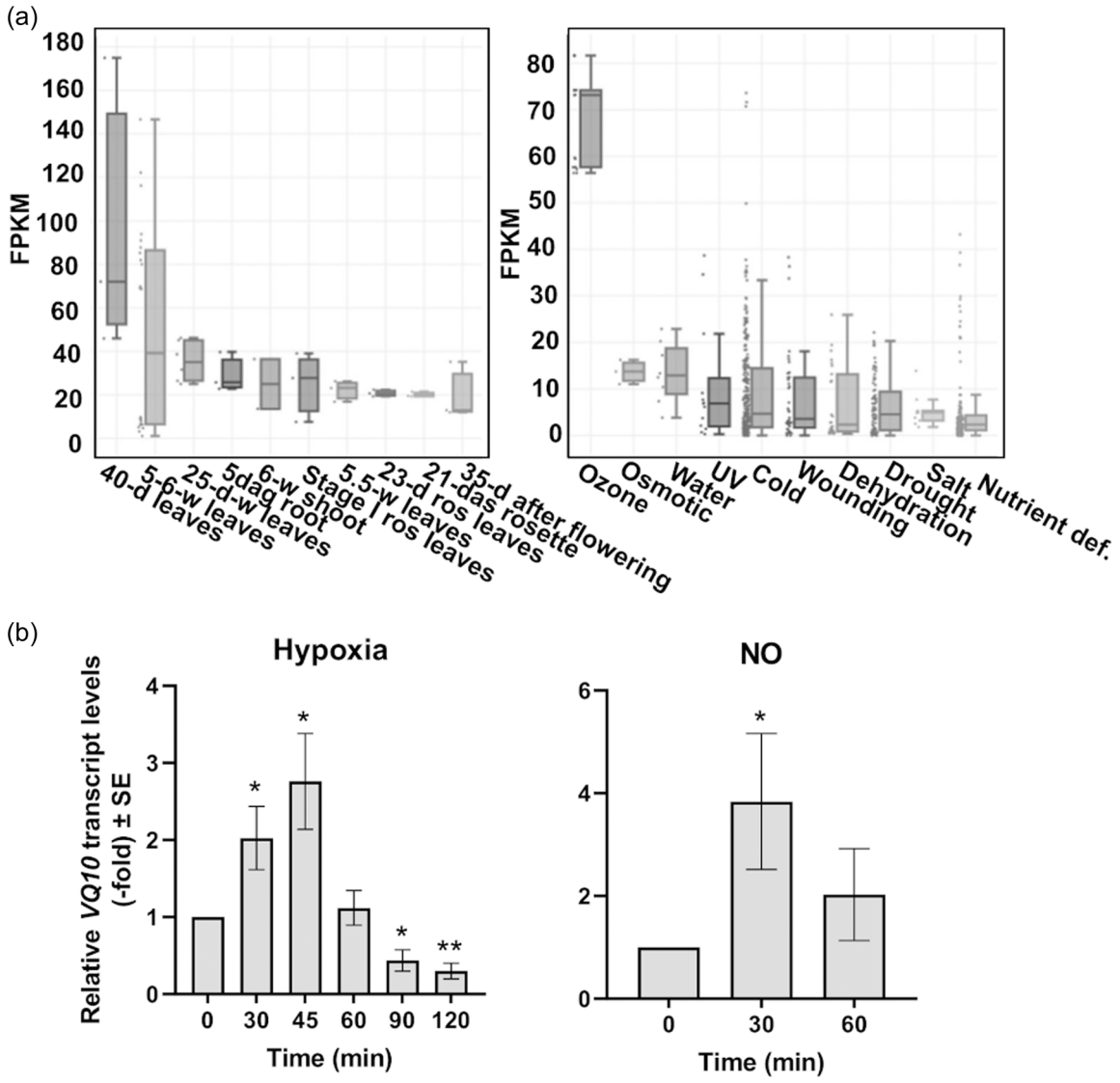

FIGURE 1 Developmental and stress factors upregulating *VQ10* expression. (a) In silico search for conditions where *VQ10* expression was upregulated in public RNA-Seq data was performed with Arabidopsis RNA-Seq Database. (b) Relative *VQ10* transcript levels were analysed by RT-qPCR from three independent RNAs isolated at the indicated times after plants were exposed to 1% O_2 under darkness (hypoxia, left panel) or after application of a 300 ppm nitric oxide pulse (NO, right panel). Values are the mean ± standard error and the statistical significance assessed by *t* test comparing each condition with untreated control at 0 time. $^{*}p < 0.05$ and $^{**}p<0.005$.

cluster included *At1g78430*, *At1g78450* and *At1g78490*. A closer look of the RNA-Seq data allowed identifying that these repressed clusters comprised nine loci between *At1g78420* and *At1g78500* with very few, but some reads (Supporting Information: Figure S1a), thus indicating these loci are not affected by a deletion caused by the T-DNA insertion but downregulated by an unknown regulatory factor which may be related to VQ10. We have confirmed that the two more closely genes located downstream *VQ10*, *DA2* and *RIP2*, which code for an E3 ubiquitin ligase and a Rho protein effector, respectively, were expressed though downregulated in *vq10-H* compared to wild-type plants (Supporting Information: Figure S1b). Among the most downregulated genes in *vq10-H* plants we found *MRD1* (*Mto 1 responding down 1*) gene, which was downregulated in the *mto1-1* mutant that overaccumulates soluble methionine and that is involved in promoting salicylic acid-mediated defense (Singh et al., 2022); *HEI10* (homologue of *Human Enhancer of cell Invasion no.10*), which codes for a ZMM protein required for class I crossover formation (Morgan et al., 2021) and *Qua-Quine Starch* (*QQS*), which codes for a relevant regulator of starch content that is presumably involved in modulating carbon/nitrogen allocation in Arabidopsis (Li et al., 2015) through a process where phytochrome interaction factors (PIF) transcription factors play a relevant role (Lee et al., 2023). We confirmed by qRT-PCR from independent replicate samples that both *QQS* and *HEI10* genes were strongly down-regulated in *vq10-H* compared to wild-type plants (Supporting Information: Figure S2a). We also confirmed that the reduced *QQS*

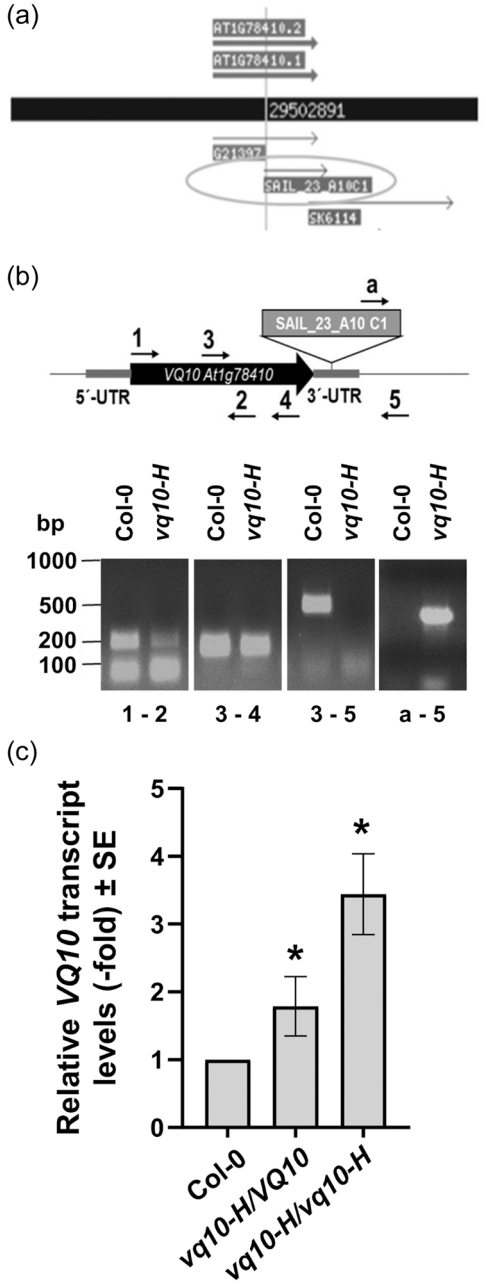

FIGURE 2 Molecular characterisation of *vq10-H* hypermorphic mutant. (a) Annotation of T-DNA insertion SAIL_A23_A10C1 in the SIGnAL T-DNA Express site (http://signal.salk.edu/cgi-bin/tdnaexpress). (b) PCR-based genotyping of the T-DNA insertion in the 3′-UTR region of the *At1g78410* locus was performed by using specific oligonucleotides 1–5 and a (Supporting Information: Table S1). Ethidium bromide-stained DNA in agarose gels is shown for each genotype and primer combinations with DNA molecular mass marker positions in the left side. (c) *VQ10* transcript was analysed by RT-qPCR from three independent RNAs isolated from plants of the indicated genotypes. Values are the mean ± standard error and the statistical significance assessed by *t* test comparing each condition with untreated control at 0 time. $^*p < 0.05$.

expression correlated with slightly higher endogenous levels of starch in *vq10-H* plants compared to wild-type plants (Supporting Information: Figure S2b). *ICME-like 2* (*ICMEL2*), which is also downregulated in *vq10-H* plants, codes for isoprenylcysteine methylesterases (ICME) that demethylate prenylated proteins that seems to be involved in regulating ABA sensitivity and signalling (Lan et al., 2010). It is also worth mentioning that *PER15*, *PER44* and *PER49* genes coding for peroxidases presumably involved in oxidative stress-related responses, are also downregulated in normoxic *vq10-H* plants. Only few genes, *PCR1*, *PRA1F4* and *PI4KG3*, are upregulated in normoxic *vq10-H* plants (Table 1). These genes code for proteins related to cadmium resistance, prenylated Ras-associated binding (RAB) acceptor involved in endomembrane protein trafficking (Lee et al., 2017), and phosphoinositide 4-kinase involved in abiotic stress responses and floral transition (Akhter et al., 2016), respectively. *PI4KG3* is also upregulated and *QQS*, *RIP4* and *MRD1* downregulated in *vq10-H* compared to Col-0 plants under hypoxia (Table 2), thus suggesting these genes are regulated by VQ10 independently of the oxygen availability conditions. In turn, *PRA1F4*, which was strongly upregulated under normoxia in *vq10-H* plants, was the most downregulated gene under hypoxia (Table 2). PRA1F4 seems to be involved in the exit of many post-Golgi proteins from the Golgi apparatus (Lee et al., 2017), thus suggesting VQ10 might play a role in regulating endomembrane protein trafficking in opposite ways depending on the O_2 availability.

In contrast to the limited impact of *vq10-H* mutation on gene expression, the comparison of hypoxia versus normoxia in Col-0 and *vq10-H* plants showed around 1000 DEGs upregulated and another 1000 DEGs downregulated (Figure 3c). It is worth mentioning that around 60% of the upregulated and 40% of the downregulated DEGs in response to hypoxia were common in Col-0 and *vq10-H* plants (Figure 3c), thus pointing to a central core of invariant genes regulated by hypoxia in both genotypes and therefore not presumably regulated by VQ10. Nevertheless, several hundred genes were specifically upregulated or downregulated by hypoxia in Col-0 or *vq10-H* plants, these representing potential targets of regulation by VQ10. Among the 267 genes that were upregulated by hypoxia in Col-0 plants but not in *vq10-H* plants, GO analysis pointed to a significant overrepresentation of genes belonging to the functional categories related to responses to light intensity, drought and ABA (Supporting Information: Table S3). Among the 418 genes that were downregulated by hypoxia in Col-0 plants but not in *vq10-H* plants, the glucosinolate biosynthesis and response to insects as well as DNA-templated DNA replication, cell differentiation, plant epidermis development and root morphogenesis were significantly overrepresented (Supporting Information: Table S3). Genes involved in these functional categories would be potentially repressed by hypoxia but activated by VQ10. Regarding the 267 and 354 genes that were upregulated or downregulated, respectively, by hypoxia in *vq10H* but not in Col-0 plants, meaning hypoxia-regulated genes with responses

TABLE 1 Differentially expressed genes in *vq10-H* versus wild-type Col-0 plants in normoxia.

Gene ID	log2 (N_vq10/N_Col)	Qvalue (N_vq10/N_Col)	AGI	Gene symbol	Annotation
838053	20.76613368	1.93E−04	AT1G14880	PCR1	Plant cadmium resistance 1 mRNA binding
820580	18.98297671	0.001731463	AT3G13710	PRA1F4	PRA1 family protein F4
832491	3.181450538	5.89E−22	AT5G24240	PI4KG3	Phosphatidylinositol 4-kinase gamma 3
844177	2.579970839	1.81E−05	AT1G78410	VQ10	VQ motif-containing protein 10
833584	1.063863295	0.025503809	AT5G35940	JAL41	Jacalin-related lectin 41
824787	0.971907451	1.56E−10	AT3G56210	AT3G56210	ARM repeat superfamily protein
837385	0.945767329	0.00215803	AT1G08630	THA1	Probable low-specificity L-threonine aldolase 1
814893	0.911530596	3.58E−12	AT2G03640	AT2G03640	Nuclear transport factor 2 (NTF2) family protein with RNA binding (RRM-RBD-RNP motifs) domain-containing protein
825789	0.835978855	7.12E−04	AT4G04570	CRK40	Cysteine-rich receptor-like protein kinase 40
837543	0.740397434	5.34E−04	AT1G10070	BCAT2	Branched-chain-amino-acid aminotransferase 2, chloroplastic
839953	0.553914531	0.028722471	AT1G30730	AT1G30730	Berberine bridge enzyme-like 11
824247	−0.752568288	6.78E−10	AT3G50830	COR413PM2	Cold-regulated 413 plasma membrane protein 2
830433	−1.025644655	0.003607343	AT5G05500	AT5G05500	Pollen Ole e 1 allergen and extensin family protein
828707	−1.068403682	0.003945081	AT4G26010	PER44	Peroxidase 44
829795	−1.083781242	6.85E−05	AT4G36430	PER49	Peroxidase 49
822298	−1.089600344	0.006485982	AT3G26830	CYP71B15	Bifunctional dihydrocamalexate synthase/camalexin synthase
816328	−1.09788076	0.011702354	AT2G18150	PER15	Peroxidase 15
830378	−1.097984617	0.02263454	AT5G04960	PME46	Probable pectinesterase/ pectinesterase inhibitor 46
821191	−1.587335424	0.009483399	AT3G02410	ICMEL2	Probable isoprenylcysteine alpha-carbonyl methylesterase ICMEL2
828367	−2.023800483	2.60E−09	AT4G22710	CYP706A2	Cytochrome P450 - like protein
842720	−2.030903491	0.009054174	AT1G64160	DIR5	Dirigent protein 5
841784	−2.234199922	4.69E−24	AT1G53490	HEI10	E3 ubiquitin-protein ligase CCNB1IP1 homologue
822807	−3.542788923	3.23E−29	AT3G30720	QQS	Protein QQS
844179	−4.406385183	3.58E−12	AT1G78430	ICR4/RIP4	Interactor of constitutive active ROPs 4
844181	−4.600771165	1.80E−04	AT1G78450	AT1G78450	Uncharacterised protein
841783	−5.549316257	3.80E−69	AT1G53480	MRD1	Mto 1 responding down 1

TABLE 2 Differentially expressed genes in *vq10-H* versus wild-type Col-0 plants under hypoxia.

Gene ID	log2 (H_vq10/H_Col)	Qvalue (H_vq10/H_Col)	AGI	Gene Symbol	Annotation
28721171	7.079812613	1.73E−04	AT5G17522	AT5G17522	Phosphoglucosamine mutase family protein
832491	2.946139166	1.06E−06	AT5G24240	PI4KG3	Phosphatidylinositol 4-kinase gamma 3
844177	2.608878402	0.040576348	AT1G78410	VQ10	VQ motif-containing protein 10
841143	1.990209844	0.044361776	AT1G47395	AT1G47395	At1g47390_positive regulation of iron ion transport
825789	1.789238638	5.86E−06	AT4G04570	CRK40	Cysteine-rich receptor-like protein kinase 40
833584	1.395578323	1.39E−04	AT5G35940	JAL41	Jacalin-related lectin 41
838211	1.386767786	5.67E−06	AT1G16410	CYP79F1	Dihomomethionine N-hydroxylase
842897	1.33059402	2.40E−04	AT1G65860	FMOGS-OX1	Flavin-containing monooxygenase FMOGS-OX1
824787	1.241749284	2.15E−15	AT3G56210	AT3G56210	ARM repeat superfamily protein
6241166	1.118719896	0.006955817	AT1G24881	AT1G24881	F-box/kelch-repeat protein
827936	1.010923172	0.048858445	AT4G00970	CRK41	Cysteine-rich receptor-like protein kinase 41
822167	0.982167204	0.040576348	AT3G25760	AOC1	Allene oxide cyclase 1, chloroplastic
820901	0.975593159	2.25E−05	AT3G16530	AT3G16530	Lectin-like protein
821508	0.828590691	0.03811801	AT3G19710	BCAT4	Methionine aminotransferase BCAT4
824625	0.72698753	0.040576348	AT3G54600	DJ1F	DJ-1 protein homologue F
827011	0.688209597	7.86E−04	AT4G13770	CYP83A1	Cytochrome P450 83A1
824247	−0.812677938	9.31E−05	AT3G50830	COR413PM2	COR413-PM2
821017	−1.669837325	6.88E−04	AT3G17520	AT3G17520	Late embryogenesis abundant protein (LEA) family protein
839408	−2.553669157	0.024218691	AT1G03790	TZF4/SOM	Zinc finger CCCH domain-containing protein 2
822807	−3.506653821	5.04E−23	AT3G30720	QQS	Protein QQS
844185	−3.561238151	1.69E−05	AT1G78490	CYP708A3	CYP708A3
844179	−3.593109435	5.86E−06	AT1G78430	ICR4/RIP4	Interactor of constitutive active ROPs 4
841783	−6.820621928	4.72E−39	AT1G53480	MRD1	Mto 1 responding down 1
820580	−6.936168591	2.20E−04	AT3G13710	PRA1F4	PRA1 family protein F4

that would be potentiated or repressed by VQ10, we found an statistical overrepresentation of proton motive force-driven ATP synthesis, flavonoid metabolic process as well as responses to wounding, lipid, oxygen-containing compound and hormones among upregulated genes (Supporting Information: Table S3). Cellular metal ion homoeostasis, root morphogenesis and plant epidermis development were overrepresented among downregulated genes (Supporting Information: Table S3).

3.3 | Nontranscriptional regulatory functions of VQ10 protein

The limited transcriptional regulatory impact of the enhanced *VQ10* expression in the hypermorphic *vq10-H* mutant over wild-type plants suggest that the regulation exerted by this protein might be preferentially exerted at nontranscriptional level. In fact, it was previously reported that VQ10 was one of the few proteins of the Arabidopsis VQ protein family that did not bind DNA and was unable to activate or represses a transcriptional reporter (Jing & Lin, 2015). An in silico analysis of VQ10 protein based on the predictive algorithms PPRInt (https://webs.iiitd.edu.in/raghava/pprint/submit.html) and DRNApred (http://biomine.cs.vcu.edu/servers/DRNApred/) point to VQ10 as a potential RNA-binding protein (Supporting Information: Figure S3). It has been extensively reported that RNA-binding proteins act frequently by regulating alternative splicing (AS) in plants (Meyer et al., 2015) as well as protein translation (Wang et al., 2023). VQ10 functional activities might then be related to the regulation of RNA stability, location or metabolic processing. To check whether VQ10 affect AS, RNA-Seq data were interrogated for alternative spliced transcripts. Data were analysed to identify skipped exons (SE), retained introns (RI), mutually exclusive exons (MXE) and alternative 5′ or 3′splice site (A5SS or A3SS). Figure 4 summarises the AS events found in *vq10-H* and Col-0 genotypes comparisons under

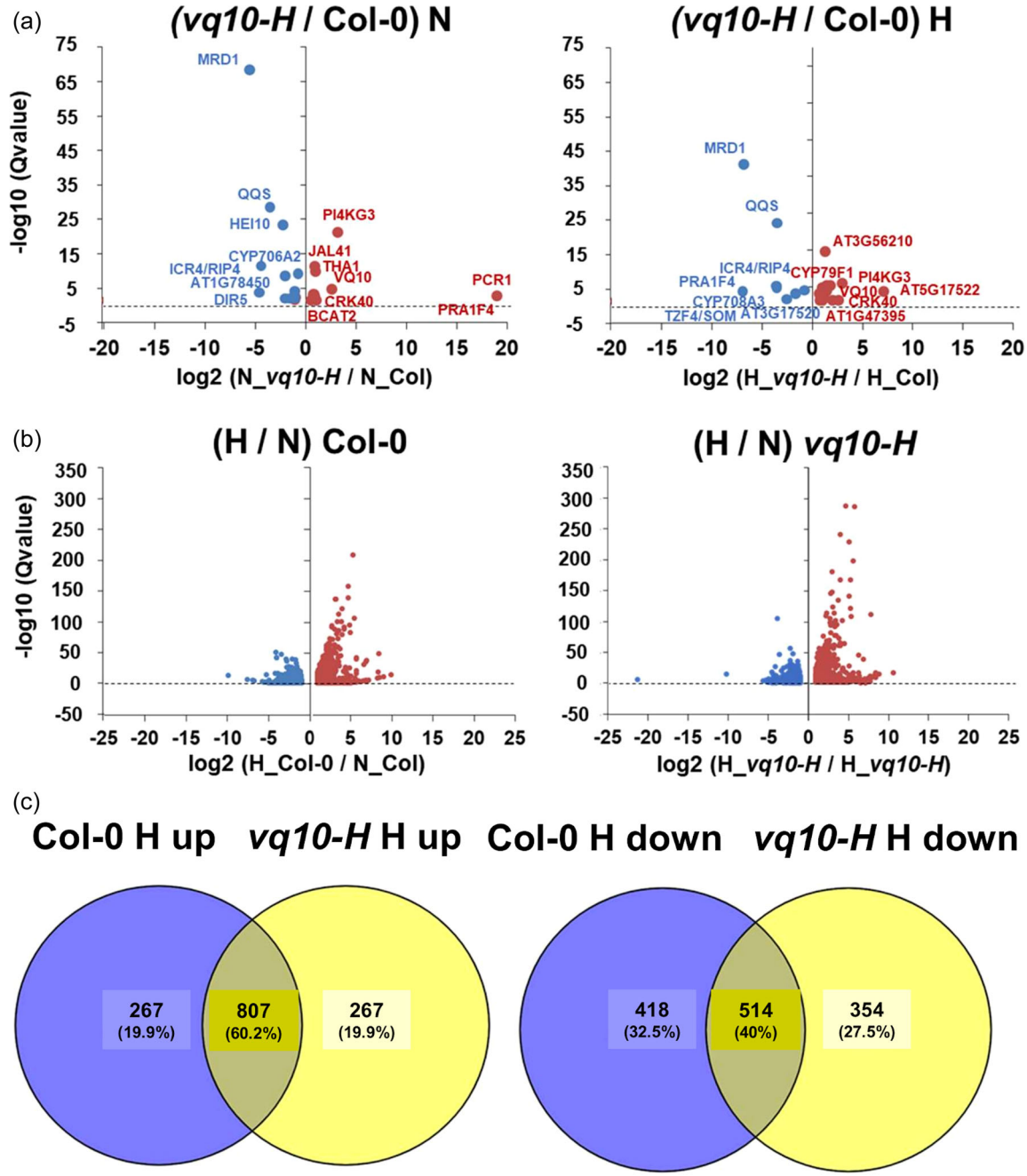

FIGURE 3 Genome-wide transcriptome analysis by RNA-Seq comparing wild type versus *vq10-H* mutant plants. Volcano plots showing: (a) differentially expressed genes (DEGs) upregulated (red) and downregulated (blue) identified when compared *vq10-H* to Col-0 plants under normoxia (N; left panel) or hypoxia (H; right panel). (b) Upregulated (red) and downregulated (blue) DEGs identified when hypoxic versus normoxic Col-0 (left panel) and *vq10-H* plants (right panel). (c) Venn diagrams showing the intersection between hypoxia upregulated (left plot) and downregulated (right plot) genes in Col-0 (blue) and *vq10-H* (yellow) plants.

normoxia or hypoxia. Gene targets of the significantly differential AS events and the corresponding statistics are included in Supporting Information: Table S4. Under normoxia, single significant differential A5SS, A3SS and SE events in *PTP1*, *AGL42* and *AT5G41690*, and seven RI in *magnesium transporter 7* (*MGT7*), *Agamous-Like42* (*AGL42*), *O-fucosyltransferase 4* (*OFUT4*), *Guanylate kinase 1* (*GK1*), *ABC transporter A family member 8* (*ABCA8*), *FTSH protease 8* (*FTSH8*) and *AT1G56520* genes were identified (Supporting Information: Table S4). Under hypoxia, more differential AS events with statistical significance were identified when Col-0 versus *vq10-H* plants were compared. Two A3SS in *sister chromatid cohesion 1 protein 2* (*SYN2*) and *cytochrome c oxidase subunit 5C* (*AT5G61310*) and seven A5SS, three of them in *cyclin-dependent kinase-activating kinase assembly factor-related* (*AT4G30820*) and the other four in *type I inositol polyphosphate*

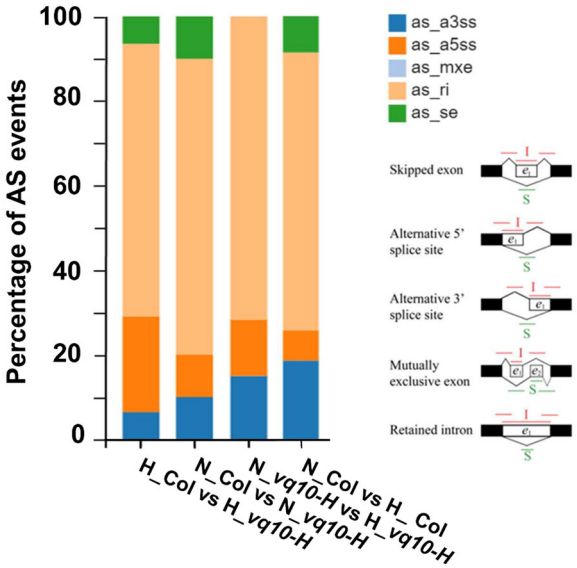

Compare_group	A5ss	A3ss	Mxe	ri	se	total
H_Col-vs-H_*vq10-H*	7	2	0	20	2	31
N_Col-vs-N_*vq10-H*	1	1	0	7	1	10
N_*vq10-H*-vs-H_*vq10-H*	8	9	0	43	0	60
N_Col vs H_ Col	5	13	0	46	6	70

FIGURE 4 Identification of differential alternative splicing events occurring when comparing Col-0 and *vq10-H* plants under normoxia or hypoxia as well as normoxia versus hypoxia in Col-0 plants. Skipped exons (SE), retained introns (RI), mutually exclusive exons (MXE) and alternative 5′or 3′ splice site (A5SS or A3SS) were analysed. Top panel shows the percentage of each alternative splicing type,and the total number of events are indicated in the box below.

5-phosphatase 10 (*IP5P10*), *serine/threonine-protein phosphatase 5* (*PAPP5*), *ADP-ribosylation factor 2-B* (ARF-2A) and *TMPIT-like protein* (*AT4G10430*) as well as two SE events in *AT5G44565* and *AT4G30820* genes were identified under hypoxia (Supporting Information: Table S4). The largest number of AS events under hypoxia corresponded to RI events, which were identified in 20 different target genes (Supporting Information: Table S4). Some of them targeted genes coding for proteins with relevant regulatory functions such as the transcription factors NFYB10 and bHLH23 or the regulatory protein RAPTOR2, and a couple of cell cycle-related genes coding for SHUGOSIN2 and a cyclin-dependent kinase-activating kinase assembly factor (Supporting Information: Table S4). The analysis of AS in wild-type Col-0 plants in hypoxic versus normoxic plants showed that 70 differential AS events were identified (Figure 4), further supporting the relevance of AS in regulating gene expression under hypoxia. Remarkably, *AGL42* and *MGT7* genes were the only loci undergoing differential AS when compared normoxic Col-0 versus *vq10-H* plants and normoxic versus hypoxic Col-0 plants (Supporting Information: Table S4). Among genes showing differential AS when compared hypoxic Col-0 versus *vq10-H* plants, *AT4G30820* coding for a cyclin-dependent kinase-activating kinase assembly factor-related protein, *NFYB10* and *BHLH23* coding for transcription factors, and *AT3G54510*, *AT2G43465*, *AT3G65685* and *AT4G02550* coding for hyperosmolarity-gated Ca^{2+} channel 2.5, an RNA-binding ASCH domain protein, a UDP-glucosyltransferase, and an unknown protein, respectively, were also differentially spliced in hypoxic versus normoxic wild-type plants (Supporting Information: Table S4).

3.4 | Developmental and stress-related phenotypes of *vq10-H* plants

To assess whether the potential developmental phenotypes of *vq10-H* plants were associated to the enhanced *VQ10* expression, we generated transgenic *VQ10ox* plants overexpressing *VQ10* gene under the *35S* promoter leading to high overexpression around two orders of magnitude above that detected in *vq10-H* plants (Supporting Information: Figure S4a), which we used together with the hypermorphic mutant. We checked that the strong down-regulation of *DA2* and *RIP2* gene expression detected in *vq10-H* plants (Supporting Information: Figure S1) was also detected in *VQ10ox* plants (Supporting Information: Figure S4b), thus suggesting the regulatory effects detected on the hypermorphic mutant was dependent on the enhanced *VQ10* expression. The phenotypic characterisation of *vq10-H* and *VQ10ox* plants allowed identifying root growth-related alterations. Figure 5a shows that the enhanced *VQ10* expression either in the hypermorphic *vq10-H* mutant or in overexpressing transgenic plants correlated with increased growth of the primary root during the first 3 days after germination. The increased growth was accompanied by enlarged root meristem in *vq10-H* plants but not in the *VQ10ox* plants, which instead developed shorter meristems (Figure 5b). The measurement of cell length in the first cells in the root elongation zone, showed that *vq10-H* and *VQ10ox* roots displayed enhanced cell elongation (Figure 5c), thus likely responsible for the overall longer root phenotype. Nevertheless, in the hypermorphic mutant plants, the enlarged root meristem was likely due to the augmented cell division rate in the meristem as demonstrated by the more intense and wider β-glucuronidase staining in *cycB1:GUS* cell division reporter plants in the roots of *vq10-H* compared to Col-0 background (Figure 5d). In turn, the cell division rate was not altered in *vq10-H* shoots (Figure 5e). Given the described functional interaction between VQ10 and WRKY33 (Cheng et al., 2012), we checked the GUS staining pattern in roots and shoots of *cycB1:GUS* in the *wrky33* background. Enhanced GUS staining was detected both in roots and shoots (Figure 5e,f), thus indicating WRKY33 negatively regulated cell division in both meristematic regions while VQ10 is a positive regulator in roots (Figure 5g). It may also happen that in shoots the enhanced *VQ10* expression was not enough to overcome the strong repression exerted by WRKY33 (Figure 5g), thus allowing strong cell division rates when WRKY33 is absent such as in the *wrky33* mutant plants. Work on VQ proteins in plants during the last decade allowed proposing that these proteins act as regulatory factors of gene

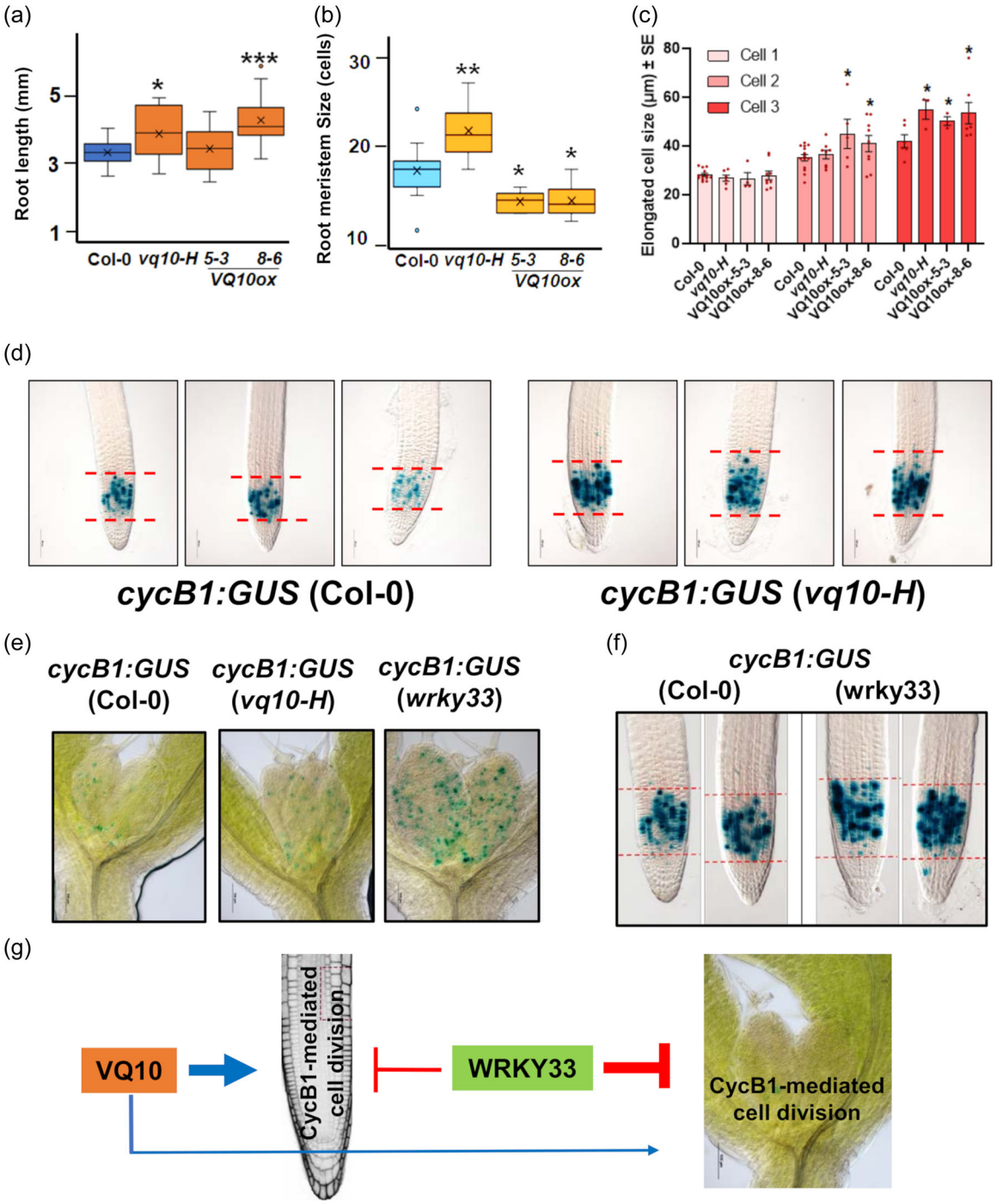

FIGURE 5 Primary root elongation, size of root meristem and cell division rate in Col-0, *vq10-H*, *VQ10ox* overexpressing transgenic lines, and *wrky33* plants. (a) The length of the primary roots of the indicated genotypes was measured in vertically grown plants by 3 days after seed germination. Box plots represent values from around 20 roots per genotype with the median value indicated by x. (b) The size of the root meristem was calculated from propidium iodide-stained roots from 4-day-old plants that were visualised by confocal microscopy and photographed. Box plots represent values from three independent experiment with 8–15 individuals per genotype and experiment. Statistical significance in (a, b) was analysed by *t* test comparing each genotype to Col-0. $^{*}p < 0.05$, $^{**}p < 0.005$, and $^{***}p < 0.001$. (c) Size of the first elongated cells in the root elongation zone of the indicated genotypes. Values are the mean ± SEM of four to eight replicates with *corresponding to $p < 0.05$. (d) Cell division was monitored by β-glucuronidase (GUS) staining in roots of *cycB1:GUS* plants in Col-0 and *vq10-H* backgrounds. Three representative images per genotype are shown. Cell division in shoots (e) or roots (f) of the indicated genotypes was monitored by GUS staining. Dotted lines represent the limits of GUS staining in root meristem in (c, e). (g) Schematic diagram showing the opposite regulation on cell division in meristems exerted by VQ10 and WRKY33. Arrows and blunt-ended lines represent activation and repression, respectively. The thickness of the lines is proportional to the effect caused.

expression in tight coordination with WRKY transcription factors (Cheng et al., 2012; Weyhe et al., 2014). Particularly, it was previously reported that the simultaneous overexpression of *VQ10* and *WRKY33* genes led to severe reduction in the rosette size of double overexpressing transgenic plants, while single *VQ10* or *WRKY33* overexpressing plants had largely normal sizes at mature stages (Cheng et al., 2012). To analyse whether the cell division-related phenotypes associated to the enhanced *VQ10* expression in *vq10-H* plants were dependent or not on WRKY33 function, *vq10-H* plants were crossed to *wrky33* mutant plants. The characterisation of the progeny yielded two important results, no double homozygous plants could be identified after genotyping the F2, F3 and F4 progenies; and a strong shoot phenotype of dwarf chlorotic plants with curly and small leaves segregated in each population, correlating with genotypes combining homozygous *wrky33/wrky33* mutant with heterozygous *VQ10/vq10-H* or homozygous *vq10-H/vq10-H* and heterozygous *WRKY33/wrky33* (Figure 6a). No such phenotypes were observed for any of the single homozygous parental plants. We

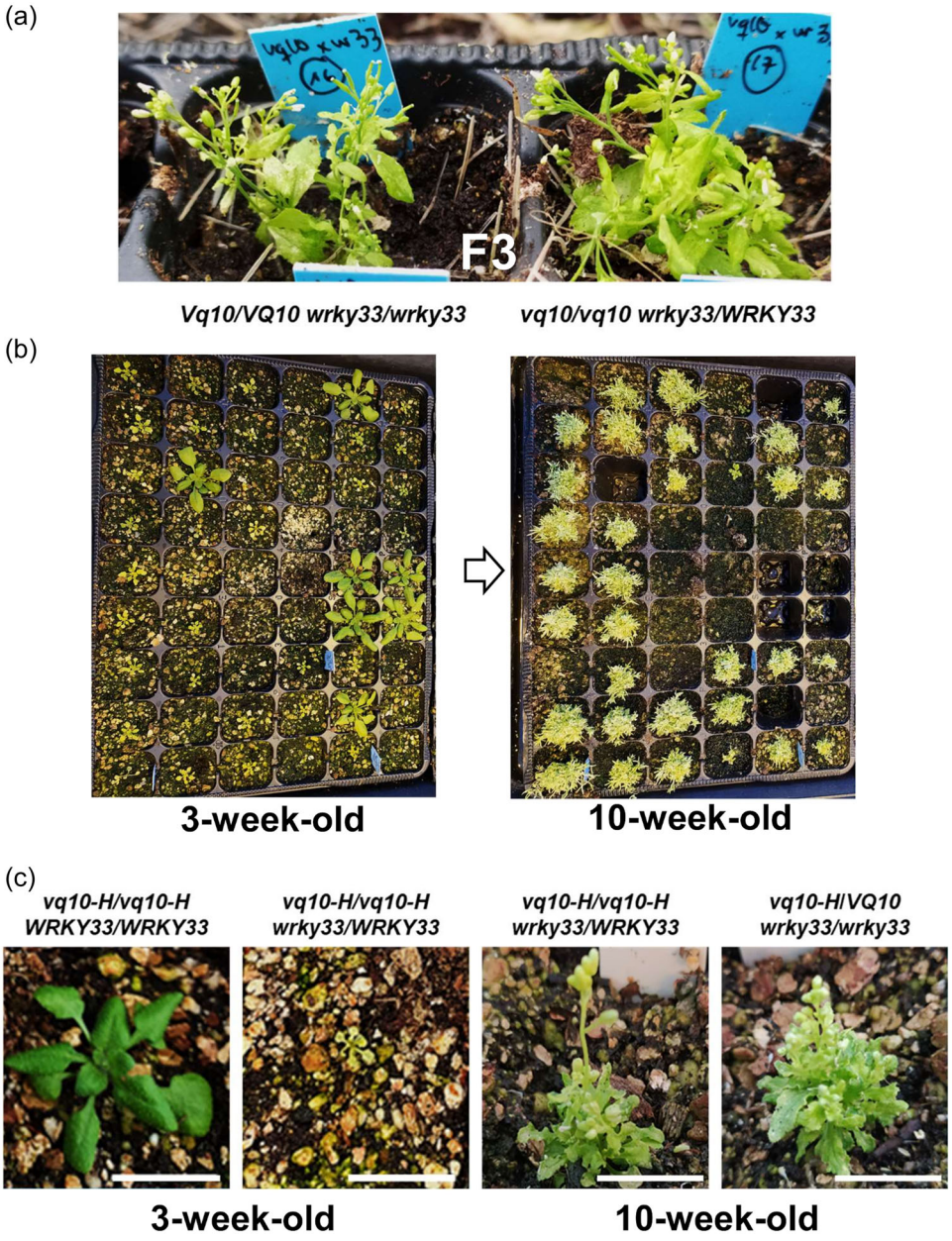

FIGURE 6 Severe shoot growth phenotype in *vq10-H* plants with enhanced *VQ10* expression in a *wrky33* knock-out background. (a) Individual plants of an F3 segregating population of the *vq10-H* × *wrky33* genetic cross showing dwarf curled phenotype with the indicated homozygous/heterozygous genotypes were selected to generate F4 seed populations. (b) Plants of the F4 progeny from homozygous heterozygous parental plants displaying segregating dwarf curled phenotype at 3 weeks (left panel) and by 10 weeks after removal of plants with wild-type phenotype (right panel). No double homozygous mutant was identified in either F3 or F4 populations. (c) Enlarged images of individual F4 plants with the indicated genotypes grown for 3 or 10 weeks as indicated. Size bars correspond to 1 cm.

selected and grown F3 individuals of both genotypes (Figure 6a) to produce F4 seeds that were sown and grown. Many plants developed the altered phenotype with homozygous/heterozygous genotypes (Figure 6b) similar to that of F3 plants, and again none of them was double homozygous plants. These data point to VQ10 as a relevant regulator of shoot growth in tight functional interaction with WRKY33 acting on cell division in meristems.

Transcriptome data revealed several DEGs coding for peroxidases that were downregulated in normoxic *vq10-H* plants (Table 1). We tested the sensitivity of *vq10-H* seeds to the oxidative stress triggered by treatment with methyl viologen (paraquat). Figure 7a shows that *vq10-H* seeds were significantly more resistant to oxidative stress than wild-type seeds, with around 50% of *vq10-H* seeds germinating at 0.1 mM paraquat while only 5% of the Col-0 seeds germinated by 96 h under this oxidative condition. By 96 h at 0.2 mM paraquat very few Col-0 seeds (less than 3%) but more than 30% of the *vq10-H* seeds germinated (Figure 7). The enhanced tolerance of seeds to oxidative stress seems to be due to the upregulation of *VQ10* gene as similar enhanced tolerance as detected for *vq10-H* seeds was also detected in seeds of transgenic overexpressing *VQ10ox* lines (Figure 7).

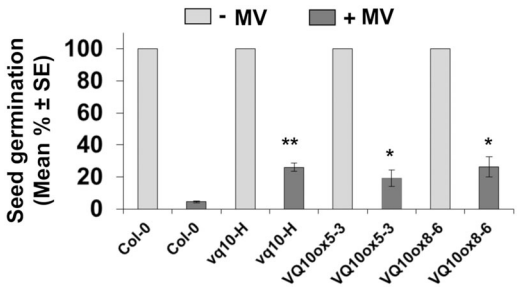

FIGURE 7 Tolerance to oxidative stress of Col-0, *vq10-H* and *VQ10ox* seed germination. Seed germination of the indicated genotypes either treated with 0.1 mM methyl viologen (MV) or untreated (MV 0) as control. Seed germination, as indicated by radicle protrusion, was calculated at Day 5 after sowing from three independent experiments each with 10–30 seeds per genotype and condition. The statistical significance was assessed by *t* test comparing each treated genotype with treated Col-0. $^{*}p < 0.05$ and $^{**}p < 0.005$.

In addition to the enhanced tolerance to oxidative stress of *vq10-H* and *VQ10ox* seeds, we also tested the sensitivity of wild type, hypermorphic mutant and overexpressing plants to exogenous NO. By performing hypocotyl elongation assays under darkness for 4 days in the presence of exogenously supplied NO compared to untreated controls, around 15% hypocotyl shortening was detected in *vq10-H* and 25% in VQ10ox plants, which was significantly less than the 45% shortening detected in NO-treated Col-0 hypocotyls (Figure 8), thus suggesting *vq10-H* and *VQ10ox* plants tolerated better the nitro-oxidative stress caused by NO maybe because VQ10 represses NO sensing or perhaps because it helps in dealing with reactive oxygen and nitrogen species.

As VQ10 was upregulated at short times after hypoxia (Figure 1b), we tested whether the hypoxia-triggered upregulation of hypoxia marker genes such as *lateral boundaries 41* (*LBD41*), (*pyruvate decarboxylase 1* (*PDC1*), *alcohol dehydrogenase 1* (*ADH1*) and *L-lactate dehydrogenase* (*LDH*) were altered in *vq10-H* and transgenic overexpressing *VQ10ox* plants. Significant upregulation of *LBD41*, *PDC1* and *ADH1* genes was detected upon hypoxia in Col-0, *vq10-H* and *VQ10ox* plants with no significant differences between hypoxic genotypes (Figure 9). The hypoxia-induced expression of *LDH* in *vq10-H* mutant plants was like wild-type plants but lower in *VQ10ox* plants (Figure 9). Moreover, the levels of basal but not hypoxia-induced expression of *LBD41* and *PDC1* were significantly different in *vq10-H* and *VQ10ox* compared to Col-0 plants (Figure 9). In turn, no significant differences were detected in *ADH1* and *LDH* transcript levels in *vq10-H* and *VQ10ox* compared to Col-0 plants under

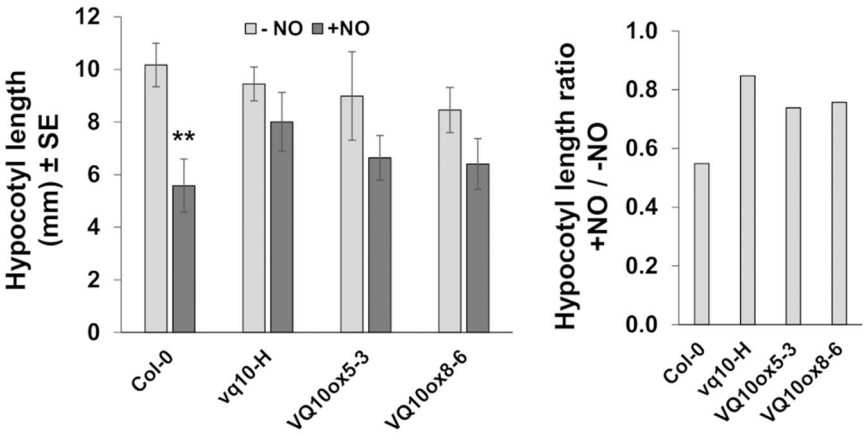

FIGURE 8 Sensitivity of wild type, *vq10-H* and *VQ10ox* hypocotyls to nitric oxide (NO). Sensitivity to NO was tested in hypocotyl shortening assays using etiolated seedlings incubated under darkness for 4 days in tight-sealed chambers containing 300 ppm +NO (dark grey) or without supplemented nitric oxide as control (−NO, light grey) as previously reported (Castillo et al., 2018). Represented values are the mean ± SE of around 25 individuals per genotype and condition. Statistical significance was assessed by unpaired *t* test comparing the NO-treated to the untreated values of the same genotype. $^{**}p < 0.005$.

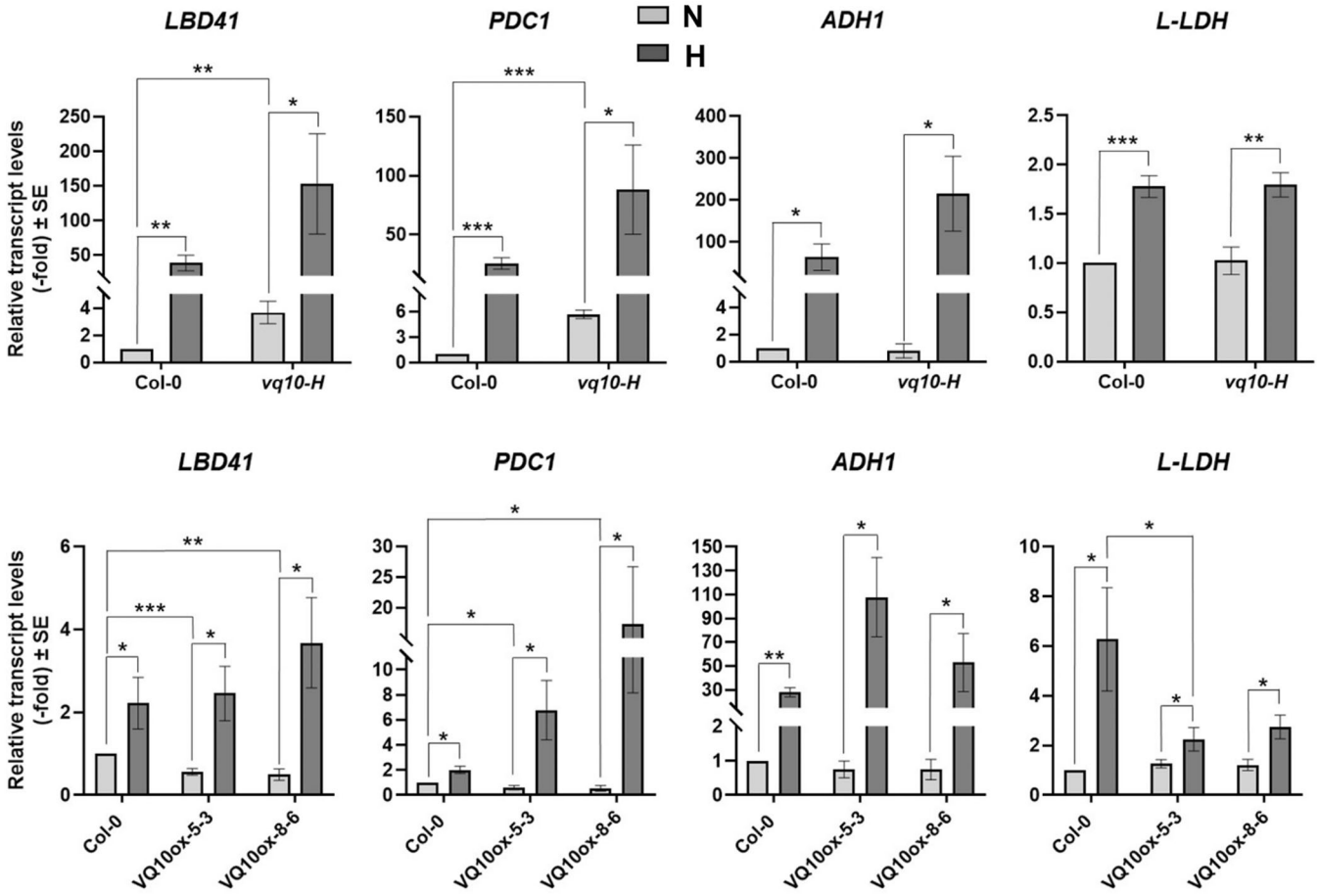

FIGURE 9 Hypoxia-triggered upregulation of marker genes in Col-0, *vq10-H* and transgenic overexpressing *VQ10ox* plants. The indicated transcripts were analysed by RT-qPCR from three independent RNAs isolated from plants of the indicated genotype and condition (N, normoxia; H, hypoxia caused by exposure to 1% O_2 for 24 h). Values are the mean ± SE and the statistical significance assessed by *t* test comparing data from genotypes in the same treatment, or different treatments for the same genotype. $^{*}p < 0.05$, $^{**}p < 0.005$, and $^{***}p < 0.001$.

normoxia (Figure 9), thus pointing to VQ10 as an activator of only *LBD41* and *PDC1* expression under normoxia but not under hypoxia. We tested whether *vq10-H* and overexpressing *VQ10ox* plants showed altered tolerance to submergence under darkness followed by reoxygenation recovery under light. The damage detected in plants after submergence/reoxygenation was quantified for any condition and genotype (Supporting Information: Figure S5). All genotypes with enhanced *VQ10* expression displayed lower tolerance to submergence and the subsequent reoxygenation recovery with increased percentage of damaged plants compared to Col-0 (Supporting Information: Figure S5). To check whether the altered tolerance to hypoxia of plants with enhanced *VQ10* expression was related to changes in the energy status of the plants, the endogenous ATP levels were quantified. No significant differences in the ATP levels were detected when compared wild type with the hypermorphic mutant or overexpressing plants either under nonstressed or NO-triggered nitroxidative stress (Supporting Information: Figure S6). We also tested whether changes in the tolerance to hypoxia/reoxygenation, oxidative stress in seeds and hyposensitivity to NO in hypocotyl elongation assays of plants with enhanced *VQ10* expression correlated with changes in the pattern of 3-nitrotyrosine modification that is an indicator of the sensitivity to nitroxidative stress. We found that the pattern of 3-nitrotyrosine containing proteins, which was strongly promoted by the exposure to NO, were not significantly different in wild type, *vq10-H* mutant or *VQ10ox* overexpressing plants (Supporting Information: Figure S7a). Moreover, although the use of free 3-nitrotyrosine is not a commonly used marker for nitroxidative stress in plants as it is for mammals, we have developed an analytical method based on UPLC-MS/MS to determine the levels of free 3-nitrotyrosine. Our results point again to a large increase in the free 3-nitrotyrosine levels upon exposure to NO, but no significant differences among genotypes either in non-stressed or NO-exposed plants (Supporting Information: Figure S7b). Between 30- and 40-fold increases in free 3-nitrotyrosine levels were detected in all NO-treated plants compared to untreated controls (Supporting Information: Figure S7b).

Since *VQ10* gene was upregulated by NO (Figure 1b) and plants with enhanced constitutive expression were less sensitive to NO than wild-type plants (Figure 8), we analysed whether the VQ10 exerted regulation might work through the function of phytoglobins, which

have been characterised as important regulators of endogenous NO levels either through direct NO scavenging or through the function of phytoglobin-NO cycle (Gupta et al., 2018). Moreover, class I phytoglobins also play a relevant regulatory role on root meristem growth (Mira et al., 2020, 2023), a phenotype we found altered in roots from plants with enhanced *VQ10* expression (Figure 5). We have tested whether enhanced *VQ10* expression affect the normoxic or hypoxia-triggered upregulation of *GLB1* gene coding for an Arabidopsis class I phytoglobin. Despite *GLB1* was strongly and similarly induced by hypoxia in our RNA-seq data of Col-0 and *vq10-H* plants (21- and 26-fold, respectively; Supporting Information: Table S2), we checked *GLB1* transcript levels by qRT-PCR from independent RNAs isolated not only from wild type and *vq10-H* plants but also from overexpressing transgenic *VQ10ox* plants, either under normoxia or hypoxia. Supporting Information: Figure S8a shows that no significant differences were found when compared the different genotypes to Col-0 under normoxia, and also that *GLB1* was strongly upregulated upon hypoxia to similar extent in all genotypes. Besides, we also checked whether altered *GLB1* expression in mutant (*glb1*) and overexpressing (*GLB1ox*) transgenic plants could alter the expression of *VQ10* gene when compared to Col-0 plants. Supporting Information: Figure S8b shows that neither under normoxia or hypoxia the levels of *VQ10* transcript in mutant *glb1* or overexpressing *GLB1ox* were significantly different to that detected in Col-0 plants.

4 | DISCUSSION

Despite VQ proteins have emerged as relevant regulators of plant responses to biotic and abiotic stresses and plant growth and development (Jiang et al., 2018), very little is known about the function of most of the Arabidopsis VQ proteins. Arabidopsis VQ10, beyond the well-characterised interaction with WRKY8 to modulate defense against Botrytis (Chen et al., 2018), and their responsiveness to NO (Castillo et al., 2018) and to hypoxia and oxidative stress (León et al., 2021), remains poorly characterised. Here we report the identification and characterisation of phenotypes associated to the enhanced *VQ10* expression in the hypermorphic *vq10-H* mutant as well as genome-wide transcriptome analysis of mutant versus wild-type plants under normoxia and hypoxia. Neither the hypoxia-triggered upregulation of marker genes (Figure 9) nor the tolerance to submergence-triggered hypoxia (Supporting Information: Figure S5) was significantly altered in *vq10-H* plants, thus suggesting a minor or not decisive involvement of VQ10 in hypoxia responses. These data would be consistent with the large group of genes that were coregulated by hypoxia in wild-type and *vq10-H* plants (Figure 3c) suggesting the existence of a core of hypoxia-responsive genes that were not modulated by VQ10. On the other hand, given the limited impact of altered *VQ10* expression on the differentially expressed transcriptome of *vq10-H* compared to Col-0 plants both under normoxia or hypoxia (Tables 1 and 2; Figure 3a,b) together with the previously reported inability of VQ10 protein to bind DNA and regulate transcription (Jing & Lin, 2015), the regulatory functions exerted by VQ10 protein should rely on other features. VQ10 protein is predicted to bind RNA (Supporting Information: Figure S3), suggesting that part of the regulatory roles exerted by VQ10 protein could be related to posttranscriptional regulation that often involve the AS of target genes (Meyer et al., 2015). A set of differentially occurring AS events were identified in the RNA-Seq analysis of *vq10-H* versus Col-0 plants (Figure 4, Supporting Information: Table S4). Among the less than 10 targets of differential AS identified in normoxic plants, different AS events were detected in *AGL42* gene that encodes a MADS box transcription factor whose expression is enriched in the QC and the stele of roots, mediated the brassinosteroid perception in the epidermis and controlled root meristem size (Hacham et al., 2011; Nawy et al., 2005). Moreover, AGL42 together with other MADS-box transcription factors promote flowering at the shoot apical and axillary meristems through a gibberellin-dependent pathway (Dorca-Fornell et al., 2011). We found that the root of *vq10-H* plants grew more actively during the early primary root elongation stage (Figure 5a) correlating with enlarged root meristem size (Figure 5b) and increased root cell division rate (Figure 5c). On the other hand, the cell division rate in the shoot of *cycB1:GUS* plants in *vq10-H* background did not differ from that detected in *cycB1:GUS* plants in Col-0 background, but it was strongly enhanced both in shoots and roots of the reporter plants in the *wrky33* knock-out background (Figure 5d,e). These findings suggest that cell division is oppositely regulated by VQ10 and WRKY33 acting as activator and repressor, respectively. In roots, the activation by VQ10 is preponderant on the repression by WRKY33 (Figure 5e). In turn, the repressor function of WRKY33 would prevail in shoots (Figure 5e), thus explaining the strong GUS staining detected in the shoot apical meristem of *cycB1:GUS* plants in *wrky33* background. However, in *VQ10ox* plants with very high levels of *VQ10* expression, the size of the root apical meristem was not larger like in *vq10-H* roots but, in turn, shorter than in wild-type roots (Figure 5b), thus suggesting a lack of WRKY33 repressing function in controlling cell division in *VQ10ox* roots. AGL42 was not differentially expressed in *vq10-H* plants (Supporting Information: Table S2) but it cannot be ruled out that the occurrence of differential AS events in *AGL42* locus in *vq10-H* plants may be somehow involved. Interestingly, the genetic cross between *vq10-H* and *wrky33* plants led to double homozygous/heterozygous mutant plants with simultaneous enhanced *VQ10* expression due to the hypermorphic double *vq10-H* mutation and downregulated *WRKY33* expression because the *wrky33* knock-out mutation. These plants developed dwarf shoots with many curly chlorotic leaves and delayed bolting (Figure 6), a phenotype that suggest a high cell proliferation in shoot meristem and that is consistent with a potential reduced AGL42 function due to the formation of alternative spliced inactive forms in *vq10-H* plants (Supporting Information: Table S4). In addition, it is worth mentioning that we identified several differential AS events in hypoxic *vq10-H* plants, including alternative 5′ spliced sites, RI and SE, that target *At4g30820* gene (Supporting Information: Table S4) coding for a cyclin-dependent kinase-activating kinase assembly factor-related

protein for which 19 different spliced forms have been identified and that is involved in the control of cell division and transcription (Umeda et al., 2005). It is tempting to propose that the VQ10-related effects on cell division in root and shoot apical meristems, described above under normoxic conditions, may be somehow potentiated under hypoxia through AS-mediated mechanisms involving phosphorylation events in different substrates.

Germination of *vq10-H* and *VQ10ox* seeds was significantly higher than wild-type seeds under oxidative stress (Figure 7), thus suggesting VQ10 may play a role in either activating antioxidant processes or in minimising the deleterious effects of reactive oxygen. However, the upregulated differential transcriptome in *vq10-H* plants did not include any gene coding for an antioxidant enzyme. The second most upregulated gene codes for the Prenylated Rab GTPase Receptor PRA1.F4 that is involved in the exit of some types of post-Golgi proteins from the Golgi apparatus (Lee et al., 2017). Interestingly, the ICME encoding gene *ICMEL2* was downregulated in *vq10-H* plants (Table 1). This enzyme demethylates prenylated proteins that seem to be involved in regulating ABA sensitivity and signalling (Lan et al., 2010) and it may thus be also relevant to regulate the function of the prenylated PRA1.F4 protein. An Arabidopsis chloroplast localised Rab GTPase protein CPRabA5e seems to be involved in regulating vesicle transport and in promoting seed germination and growth during oxidative stress (Karim et al., 2014), and another Rab GTPase AtRabG3e, which has a role in vesicle transport between the Golgi and the plasma membrane, has been shown to be induced under oxidative stress (Mazel et al., 2004). These data suggest that the VQ10 involvement in the protection against oxidative stress would not be related to the function of antioxidant enzyme encoding genes, but to the regulation of signalling pathways, such as Rab protein modulation of vesicle trafficking between intracellular compartments. Regarding this, *vq10-H* plants displayed a strong downregulation of *ICR4/RIP4* gene coding for Interactor of Constitutive active Rho GTPase of Plants (ROPs) 4 (Table 1), thus supporting the involvement of GTP-related signalling in VQ10-exerted regulation. It has been recently reported that the ROP2 GTPase participates in NO-Induced Root Shortening in Arabidopsis (Kenesi et al., 2023). We found that NO strongly upregulated *VQ10* gene (Figure 1b) and also that *vq10-H* plants were less sensitive to NO than Col-0 in shortening hypocotyl assays with etiolated plants (Figure 8), a phenotype that could also involve the participation of Rho GTPase-related signalling. It is worth mentioning that normoxic *vq10-H* plants displayed significant downregulation of three peroxidase-encoding genes (Table 1). It has been reported that mutations in rice that led to the accumulation of reactive oxygen species caused the strong downregulation of eight peroxidase-encoding genes (Li et al., 2021), and in Arabidopsis the peroxidase downregulation seems to be a signature of oxidative stress responses (Choi et al., 2019), thus suggesting *vq10-H* plants may undergo constitutive oxidative stress under normoxia. A constitutively high oxidative state of *vq10-H* plants may be the reason why *vq10-H* seeds better tolerate the application of an exogenous generator of oxidative stress such as methyl viologen (Figure 7). It is known that the QC of roots remains under hypoxic conditions, but it requires of oxidising conditions to ensure its establishment and maintenance (Jiang et al., 2003). This oxidised state may compromise mitochondrial function, the generation of energy, and some energy-consuming processes such as cell division (Jiang et al., 2006). In *vq10-H* plants the enhanced *VQ10* expression correlated with enhanced cell division in the root apical meristem (Figure 5d), but no significant differences were detected in the ATP levels when plants with enhanced *VQ10* expression were compared to wild-type plants (Supporting Information: Figure S6), thus suggesting the regulation exerted by VQ10 is uncoupled from altered mitochondria-related energy effects. Despite QC is always under hypoxia, roots still respond to imposing exogenous hypoxia and it has been reported that maize class-I phytoglobins play an essential role in protecting the QC from shifting from oxidative to reduced state under stress (Mira et al., 2020, 2023). This role is exerted through NO-mediated processes (Mira et al., 2020). In Arabidopsis, the class-I phytoglobin encoding gene *GLB1* is strongly upregulated by hypoxia and exposure to NO, and we found that it was strongly and similarly upregulated by hypoxia in *vq10-H* and Col-0 plants (Supporting Information: Table S2 and Figure S8a) and not significantly different in mutant and wild-type plants under normoxia (Supporting Information: Table S2 and Figure S8a), thus pointing to no involvement of GLB1 in VQ10-exerted regulation of cell division in roots. Alternatively, the altered expression of *GLB1* gene in mutant or overexpressing plants could act on *VQ10* expression. However, by using *glb1* mutant and *GLB1ox* overexpressing plants we found no significant alterations in *VQ10* expression compared to wild-type plants either under normoxia or hypoxia, thus suggesting GLB1 is not relevant to regulate VQ10 expression and action under the tested conditions in this work.

Another potential mechanism of action for VQ10 could be related to mitochondria-related alterations not in energy generation but in primary C metabolism. *QQS* gene coding for a key protein regulating starch metabolism was strongly downregulated in *vq10-H* plants either in normoxia or hypoxia (Tables 1 and 2; Supporting Information: Figure S2a). It has been reported that the expression of *QQS* and other starch-related genes was altered under oxidative stress conditions (Jones et al., 2016). Accordingly, *vq10-H* mutant plants contained higher levels of starch than wild-type plants (Supporting Information: Figure S2b). Noteworthy, *VQ10* transcript levels were increased around 2.0-2.5-fold in Arabidopsis *sex1-3* and *sex4-3* mutants that accumulated starch (GEO accession GSE19260). Future work will be needed to determine whether the changes in the endogenous levels of starch may be linked to altered *VQ10* gene expression and to phenotypes such as altered root growth or sensitivity to nitroxidative stress described in this article. However, starch that is stored in seeds, is the main source of energy for germination and it was documented that the starch content affect seed germination through alterations in the starch-sugars balance due to altered starch metabolism (Zhang et al., 2022). We checked whether the energy status of plants with enhanced *VQ10* expression was significantly different from wild-type plants either under

non-stressed conditions or upon nitroxidative stress caused by application of exogenous NO. No significant changes in the endogenous levels of ATP were found when compared *vq10-H* or *VQ10ox* plants to Col-0 plants under both conditions (Supporting Information: Figure S6), thus suggesting the altered tolerance to nitroxidative stress seems to be not related to the energy status of the plant. Like ATP, the levels of free and protein-bound 3-nitrotyrosine, which is a marker of nitroxidative stress, were largely increased upon exposure to NO in all the genotypes tested with no significant differences between genotypes, thus suggesting changes in tolerance to stress were not related to massive posttranslational modifications of proteins by nitration of tyrosine residues.

Findings presented here point out that VQ10 proteins is a potential integrator of developmental and stress-related cues acting as a regulatory protein through non-DNA-binding mechanisms. It is likely, though still to be demonstrated, that VQ10 regulatory actions reside mainly in the interaction with RNAs and other proteins, a hypothesis that we are already exploring. We have found that VQ10 and its close homologue VQ1 protein interact with many proteins with diverse subcellular localisation. Among these VQ10-interacting proteins, we found a significant enrichment of chloroplast proteins involved in the assembly, function and maintenance of photosystems as well as diverse enzymes participating in C, N and S metabolism. Moreover, the altered *VQ10* expression in overexpressing and amiRNA-targeted transgenic plants correlated with changes in the efficiency of photosynthesis as well as in de-etiolation and greening (manuscript in preparation). Whether regulation exerted by VQ10 protein on chloroplast function, or any other identified VQ10-interacting protein are functionally linked to the phenotypes of enhanced tolerance to oxidative stress and reduced sensitivity to NO observed in this work for *vq10-H* plants will require further experimental support, but protein–protein interaction is likely very relevant for VQ10 exerted regulation on multiple processes.

ACKNOWLEDGEMENTS

We thank Prof. Imre Somssich (Max Planck Institute for Plant Breeding Research, Germany) for sharing seeds of *wrky33* mutant, and Dr. David Alabadí (IBMCP, Valencia, Spain) for sharing cycB1:GUS transgenic seeds (Colon-Carmona et al., 1999). This work was supported by grants from the Spanish Ministry of Economy and Competitiveness and "Agencia Estatal de Investigación"/FEDER/European Union (BIO2017-82945-P and PID2020-112618GB-I00 to J. L.) and from Generalitat Valenciana/FEDER (IDIFEDER/2021/007 to J. L.). B. G. was recipient of a Ministerio de Ciencia e Innovación contract (PRE2018-086290).

CONFLICT OF INTEREST STATEMENT

The authors declare no conflict of interest.

DATA AVAILABILITY STATEMENT

The data supporting the findings of this study are openly available, and the RNA-Seq data have been deposited in GEO database with accession code GSE214887.

ORCID

José León http://orcid.org/0000-0002-7332-1572

REFERENCES

Akhter, S., Uddin, M.N., Jeong, I.S., Kim, D.W., Liu, X.M. & Bahk, J.D. (2016) Role of Arabidopsis AtPI4Kγ3, a type II phosphoinositide 4-kinase, in abiotic stress responses and floral transition. *Plant Biotechnology Journal*, 14, 215–230.

Ali, M.R.M., Uemura, T., Ramadan, A., Adachi, K., Nemoto, K., Nozawa, A. et al. (2019) The ring-type E3 ubiquitin ligase JUL1 targets the VQ-motif protein JAV1 to coordinate jasmonate signaling. *Plant Physiology*, 179, 1273–1284.

Armstrong, J., Jones, R.E. & Armstrong, W. (2006) Rhizome phyllosphere oxygenation in Phragmites and other species in relation to redox potential, convective gas flow, submergence, and aeration pathways. *New Phytologist*, 172, 719–731.

Bailey-Serres, J. & Voesenek, L.A.C.J. (2008) Flooding stress: acclimations and genetic diversity. *Annual review of plant biology*, 59, 313–339.

Bensmihen, S., To, A., Lambert, G., Kroj, T., Giraudat, J. & Parcy, F. (2004) Analysis of an activated ABI5 allele using a new selection method for transgenic *Arabidopsis* seeds. *FEBS Letters*, 561, 127–131.

Le Berre, J.Y., Gourgues, M., Samans, B., Keller, H., Panabières, F. & Attard, A. (2017) Transcriptome dynamic of Arabidopsis roots infected with *Phytophthora parasitica* identifies *VQ29*, a gene induced during the penetration and involved in the restriction of infection. *PLoS One*, 12, e0190341.

Castillo, M.C., Coego, A., Costa-Broseta, Á. & León, J. (2018) Nitric oxide responses in Arabidopsis hypocotyls are mediated by diverse phytohormone pathways. *Journal of Experimental Botany*, 69, 5265–5278.

Castillo, M.C., Sandalio, L.M., Del Río, L.A. & León, J. (2008) Peroxisome proliferation, wound-activated responses and expression of peroxisome-associated genes are cross-regulated but uncoupled in *Arabidopsis thaliana*. *Plant Cell & Environment*, 31, 492–505.

Chen, J., Wang, H., Li, Y., Pan, J., Hu, Y. & Yu, D. (2018) Arabidopsis VQ10 interacts with WRKY8 to modulate basal defense against *Botrytis cinerea*. *Journal of Integrative Plant Biology*, 60, 956–969.

Cheng, Y., Zhou, Y., Yang, Y., Chi, Y.J., Zhou, J., Chen, J.Y. et al. (2012) Structural and functional analysis of VQ motif-containing proteins in Arabidopsis as interacting proteins of WRKY transcription factors. *Plant Physiology*, 159, 810–825.

Choi, W.G., Barker, R.J., Kim, S.H., Swanson, S.J. & Gilroy, S. (2019) Variation in the transcriptome of different ecotypes of *Arabidopsis thaliana* reveals signatures of oxidative stress in plant responses to spaceflight. *American Journal of Botany*, 106, 123–136.

Clough, S.J. & Bent, A.F. (1998) Floral dip: a simplified method for Agrobacterium-mediated transformation of *Arabidopsis thaliana*. *The Plant Journal*, 16, 735–743.

Colon-Carmona, A., You, R., Haimovitch-Gal, T., & Doerner, P. (1999) Spatio-temporal analysis of mitotic activity with a labile cyclin-GUS fusion protein. *The Plant Journal*, 20, 503–508.

Considine, M.J., Diaz-Vivancos, P., Kerchev, P., Signorelli, S., Agudelo-Romero, P., Gibbs, D.J. et al. (2017) Learning to breathe: developmental phase transitions in oxygen status. *Trends in Plant Science*, 22, 140–153.

Czechowski, T., Stitt, M., Altmann, T., Udvardi, M.K. & Scheible, W. (2005) Genome-wide identification and testing of superior reference genes for transcript normalization in Arabidopsis. *Plant Physiology*, 139, 5–17.

Ding, H., Yuan, G., Mo, S., Qian, Y., Wu, Y., Chen, Q. et al. (2019) Genome-wide analysis of the plant-specific VQ motif-containing proteins in tomato (*Solanum lycopersicum*) and characterization of SlVQ6 in thermotolerance. *Plant Physiology and Biochemistry*, 143, 29–39.

Dorca-Fornell, C., Gregis, V., Grandi, V., Coupland, G., Colombo, L. & Kater, M.M. (2011) The Arabidopsis SOC1-like genes *AGL42*, *AGL71*

and *AGL72* promote flowering in the shoot apical and axillary meristems. *The Plant Journal*, 67, 1006–1017.

Garcia, D., Saingery, V., Chambrier, P., Mayer, U., Jürgens, G. & Berger, F. (2003) Arabidopsis *haiku* mutants reveal new controls of seed size by endosperm. *Plant Physiology*, 131, 1661–1670.

Gargul, J.M., Mibus, H. & Serek, M. (2015) Manipulation of MKS1 gene expression affects *Kalanchoë blossfeldiana* and *Petunia hybrida* phenotypes. *Plant Biotechnology Journal*, 13, 51–61.

Gibbs, D.J., Md Isa, N., Movahedi, M., Lozano-Juste, J., Mendiondo, G.M., Berckhan, S. et al. (2014) Nitric oxide sensing in plants is mediated by proteolytic control of group VII ERF transcription factors. *Molecular Cell*, 53, 369–379.

Gupta, K.J., Kumari, A., Florez-Sarasa, I., Fernie, A.R. & Igamberdiev, A.U. (2018) Interaction of nitric oxide with the components of the plant mitochondrial electron transport chain. *Journal of Experimental Botany*, 69, 3413–3424.

Hacham, Y., Holland, N., Butterfield, C., Ubeda-Tomas, S., Bennett, M.J., Chory, J. et al. (2011) Brassinosteroid perception in the epidermis controls root meristem size. *Development*, 138, 839–848.

Hu, P., Zhou, W., Cheng, Z., Fan, M., Wang, L. & Xie, D. (2013) JAV1 controls jasmonate-regulated plant defense. *Molecular Cell*, 50, 504–515.

Jiang, K., Ballinger, T., Li, D., Zhang, S. & Feldman, L. (2006) A role for mitochondria in the establishment and maintenance of the maize root quiescent center. *Plant Physiology*, 140, 1118–1125.

Jiang, K., Meng, Y.L. & Feldman, L.J. (2003) Quiescent center formation in maize roots is associated with an auxin-regulated oxidizing environment. *Development*, 130, 1429–1438.

Jiang, S.Y., Sevugan, M. & Ramachandran, S. (2018) Valine-glutamine (VQ) motif coding genes are ancient and non-plant-specific with comprehensive expression regulation by various biotic and abiotic stresses. *BMC Genomics*, 19, 342.

Jiang, Y. & Yu, D. (2016) The WRKY57 transcription factor affects the expression of jasmonate ZIM-domain genes transcriptionally to compromise *Botrytis cinerea* resistance. *Plant Physiology*, 171, 2771–2782.

Jing, Y. & Lin, R. (2015) The VQ motif-containing protein family of plant-specific transcriptional regulators. *Plant Physiology*, 169, 371–378.

Jones, D.C., Zheng, W., Huang, S., Du, C., Zhao, X., Yennamalli, R.M. et al. (2016) A clade-specific arabidopsis gene connects primary metabolism and senescence. *Frontiers in Plant Science*, 7, 983.

Karim, S., Alezzawi, M., Garcia-Petit, C., Solymosi, K., Khan, N.Z., Lindquist, E. et al. (2014) A novel chloroplast localized Rab GTPase protein CPRabA5e is involved in stress, development, thylakoid biogenesis and vesicle transport in Arabidopsis. *Plant Molecular Biology*, 84, 675–692.

Kenesi, E., Kolbert, Z., Kaszler, N., Klement, É., Ménesi, D., Molnár, Á. et al. (2023) The ROP2 GTPase participates in nitric oxide (NO)-induced root shortening in arabidopsis. *Plants*, 12, 750.

Kim, D.Y., Kwon, S.I., Choi, C., Lee, H., Ahn, I., Park, S.R. et al. (2013) Expression analysis of rice *VQ* genes in response to biotic and abiotic stresses. *Gene*, 529, 208–214.

Lan, P., Li, W., Wang, H. & Ma, W. (2010) Characterization, sub-cellular localization and expression profiling of the isoprenylcysteine methylesterase gene family in *Arabidopsis thaliana*. *BMC Plant Biology*, 10, 212.

Lee, M.H., Yoo, Y.J., Kim, D.H., Hanh, N.H., Kwon, Y. & Hwang, I. (2017) The prenylated Rab GTPase receptor PRA1.F4 contributes to protein exit from the Golgi apparatus. *Plant Physiology*, 174, 1576–1594.

Lee, S.W., Choi, D., Moon, H., Kim, S., Kang, H., Paik, I. et al. (2023) PHYTOCHROME-INTERACTING FACTORS are involved in starch degradation adjustment via inhibition of the carbon metabolic regulator QUA-QUINE STARCH in Arabidopsis. *The Plant Journal*, 114, 110–123. https://doi.org/10.1111/tpj.16124

Lei, R., Li, X., Ma, Z., Lv, Y., Hu, Y. & Yu, D. (2017) Arabidopsis WRKY2 and WRKY34 transcription factors interact with VQ20 protein to modulate pollen development and function. *The Plant Journal*, 91, 962–976.

Lei, R., Ma, Z. & Yu, D. (2018) WRKY2/34-VQ20 modules in *Arabidopsis thaliana* negatively regulate expression of a trio of related MYB transcription factors during pollen development. *Frontiers in Plant Science*, 9, 331.

León, J., Gayubas, B. & Castillo, M.C. (2021) Valine-glutamine proteins in plant responses to oxygen and nitric oxide. *Frontiers in Plant Science*, 11, 632678.

Li, L., Zheng, W., Zhu, Y., Ye, H., Tang, B., Arendsee, Z.W. et al. (2015) QQS orphan gene regulates carbon and nitrogen partitioning across species via NF-YC interactions. *Proceedings of the National Academy of Sciences*, 112, 14734–14739.

Li, N., Li, X., Xiao, J. & Wang, S. (2014) Comprehensive analysis of VQ motif-containing gene expression in rice defense responses to three pathogens. *Plant Cell Reports*, 33, 1493–1505.

Li, R.Q., Jiang, M., Huang, J.Z., Møller, I.M. & Shu, Q.Y. (2021) Mutations of the *Genomes Uncoupled 4* gene cause ROS accumulation and repress expression of peroxidase genes in rice. *Frontiers in Plant Science*, 12, 682453.

Li, Y., Jing, Y., Li, J., Xu, G. & Lin, R. (2014) Arabidopsis VQ MOTIF-CONTAINING PROTEIN29 represses seedling deetiolation by interacting with PHYTOCHROME-INTERACTING FACTOR1. *Plant Physiology*, 164, 2068–2080.

Mazel, A., Leshem, Y., Tiwari, B.S. & Levine, A. (2004) Induction of salt and osmotic stress tolerance by overexpression of an intracellular vesicle trafficking protein AtRab7 (AtRabG3e). *Plant Physiology*, 134, 118–128.

Meyer, K., Koester, T. & Staiger, D. (2015) Pre-mRNA splicing in plants: in vivo functions of RNA-binding proteins implicated in the splicing process. *Biomolecules*, 5, 1717–1740.

Mira, M.M., El-Khateeb, E.A., Gaafar, R.M., Igamberdiev, A.U., Hill, R.D. & Stasolla, C. (2020) Stem cell fate in hypoxic root apical meristems is influenced by phytoglobin expression. *Journal of Experimental Botany*, 71, 1350–1362.

Mira, M.M., Hill, R.D., Hilo, A., Langer, M., Robertson, S., Igamberdiev, A.U. et al. (2023) Plant stem cells under low oxygen: metabolic rewiring by phytoglobin underlies stem cell functionality. *Plant Physiology*. https://doi.org/10.1093/plphys/kiad344

Morgan, C., Fozard, J.A., Hartley, M., Henderson, I.R., Bomblies, K. & Howard, M. (2021) Diffusion-mediated HEI10 coarsening can explain meiotic crossover positioning in *Arabidopsis*. *Nature Communications*, 12, 4674.

Nawy, T., Lee, J.Y., Colinas, J., Wang, J.Y., Thongrod, S.C., Malamy, J.E. et al. (2005) Transcriptional profile of the *Arabidopsis* root quiescent center. *The Plant Cell*, 17, 1908–1925.

Pan, J., Wang, H., Hu, Y. & Yu, D. (2018) Arabidopsis VQ18 and VQ26 proteins interact with ABI5 transcription factor to negatively modulate ABA response during seed germination. *The Plant Journal*, 95, 529–544.

Perilli, S. & Sabatini, S. (2010) Analysis of root meristem size development. *Methods in Molecular Biology*, 655, 177–187.

Singh, A., Sharma, A., Singh, N. & Nandi, A.K. (2022) MTO1-RESPONDING DOWN 1 (MRD1) is a transcriptional target of OZF1 for promoting salicylic acid-mediated defense in Arabidopsis. *Plant Cell Reports*, 41, 1319–1328.

Song, W., Zhao, H., Zhang, X., Lei, L. & Lai, J. (2016) Genome-wide identification of VQ motif-containing proteins and their expression profiles under abiotic stresses in maize. *Frontiers in Plant Science*, 6, 1177.

Takahashi, H., Yamauchi, T., Rajhi, I., Nishizawa, N.K. & Nakazono, M. (2015) Transcript profiles in cortical cells of maize primary root during ethylene-induced lysigenous aerenchyma formation under aerobic conditions. *Annals of Botany*, 115, 879–894.

Umeda, M., Shimotohno, A. & Yamaguchi, M. (2005) Control of cell division and transcription by cyclin-dependent kinase-activating kinases in plants. *Plant & Cell Physiology*, 46, 1437–1442.

Voesenek, L. & Bailey-Serres, J. (2013) Flooding tolerance: O_2 sensing and survival strategies. *Current Opinion in Plant Biology*, 16, 647–653.

Voesenek, L.A.C.J. & Bailey-Serres, J. (2015) Flood adaptive traits and processes: an overview. *New Phytologist*, 206, 57–73.

Wang, A., Garcia, D., Zhang, H., Feng, K., Chaudhury, A. & Berger, F. et al. (2010) The VQ motif protein IKU1 regulates endosperm growth and seed size in Arabidopsis. *The Plant Journal*, 63, 670–679.

Wang, L., Xu, F. & Yu, F. (2023) Two environmental signal-driven RNA metabolic processes: alternative splicing and translation. *Plant, Cell & Environment*, 46, 718–732.

Weigel, D. & Glazebrook, J. (2002) *Arabidopsis: a laboratory manual*. CSLH Press.

Weyhe, M., Eschen-Lippold, L., Pecher, P., Scheel, D. & Lee, J. (2014) Ménage à trois: the complex relationships between mitogen-activated protein kinases, WRKY transcription factors, and VQ-motif-containing proteins. *Plant Signal & Behavior*, 9, e29519.

Xie, Y.D., Li, W., Guo, D., Dong, J., Zhang, Q., Fu, Y. et al. (2010) The *Arabidopsis* gene SIGMA FACTOR-BINDING PROTEIN 1 plays a role in the salicylate- and jasmonate-mediated defence responses. *Plant Cell & Environment*, 33, 828–839.

Ye, Y.J., Xiao, Y.Y., Han, Y.C., Shan, W., Fan, Z.Q., Xu, Q.G. et al. (2016) Banana fruit VQ motif-containing protein5 represses cold-responsive transcription factor MaWRKY26 involved in the regulation of JA biosynthetic genes. *Scientific Reports*, 6, 23632.

Zhang, M., Li, B., Wan, Z., Chen, X., Liu, C., Liu, C. et al. (2022) Exogenous spermidine promotes germination of aged sorghum seeds by mediating sugar metabolism. *Plants*, 11, 2853.

SUPPORTING INFORMATION

Additional supporting information can be found online in the Supporting Information section at the end of this article.

How to cite this article: Gayubas, B., Castillo, M.-C., Ramos, S. & León, J. (2023) Enhanced meristem development, tolerance to oxidative stress and hyposensitivity to nitric oxide in the hypermorphic *vq10-H* mutant in *AtVQ10* gene. *Plant, Cell & Environment*, 1–19. https://doi.org/10.1111/pce.14685